



Published in final edited form as:

Cell Chem Biol. 2016 January 21; 23(1): 183–197. doi:10.1016/j.chembiol.2015.11.010.

DNA Charge Transport: From Chemical Principles to the Cell

Anna R. Arnold¹, Michael A. Grodick¹, and Jacqueline K. Barton^{*}

Division of Chemistry and Chemical Engineering, California Institute of Technology, Pasadena CA 91125

Abstract

The DNA double helix has captured the imagination of many, bringing it to the forefront of biological research. DNA has unique features that extend our interest into areas of chemistry, physics, material science and engineering. Our laboratory has focused on studies of DNA charge transport (CT), wherein charges can efficiently travel long molecular distances through the DNA helix while maintaining an exquisite sensitivity to base pair π -stacking. Because DNA CT chemistry reports on the integrity of the DNA duplex, this property may be exploited to develop electrochemical devices to detect DNA lesions and DNA-binding proteins. Furthermore, studies now indicate that DNA CT may also be used in the cell by, for example, DNA repair proteins, as a cellular diagnostic, in order to scan the genome to localize efficiently to damage sites. In this review, we describe this evolution of DNA CT chemistry from the discovery of fundamental chemical principles to applications in diagnostic strategies and possible roles in biology.

Introduction

DNA is considered as the repository for genetic information in the cell. Structurally, individual strands of DNA consist of a phosphate-deoxyribose backbone connecting nitrogenous bases, either purines (adenine and guanine) or pyrimidines (cytosine and thymine). The nitrogenous bases of DNA are composed of aromatic rings with base pairs spaced 3.4 Å in the double helix. This structure allows the electron density of adjacent bases to overlap, resulting in π -stacking and a large measure of stabilization to the double helix. Significant structural similarity exists between stacked base pairs in DNA and the z -direction of graphite, a known conductive material. Specifically, adjacent graphene sheets are spaced at 3.35 Å (Chaban et al., 2014). The similar spacing of aromatic moieties in graphite and DNA led researchers to hypothesize that DNA could also be conductive through the overlap of adjacent π -orbitals (Figure 1). Decades of research have now established that DNA can indeed conduct charge efficiently through the π -stack of the nitrogenous bases (Grodick et al., 2015; Elias et al., 2008). Thus in addition to its role as the

^{*}to whom correspondence should be addressed at jkbaron@caltech.edu.

¹present address: Intel Corporation, Hillsboro OR 97124

Publisher's Disclaimer: This is a PDF file of an unedited manuscript that has been accepted for publication. As a service to our customers we are providing this early version of the manuscript. The manuscript will undergo copyediting, typesetting, and review of the resulting proof before it is published in its final citable form. Please note that during the production process errors may be discovered which could affect the content, and all legal disclaimers that apply to the journal pertain.

repository for genetic information, electrons as well as electron holes are readily transported through the DNA π -stack (Genereux and Barton, 2010).

As a macromolecular assembly in solution, however, DNA differs from graphite and other π -stacked solids. The bases of DNA are constantly undergoing dynamic motion on timescales from picoseconds to milliseconds, and these motions, though subtle, are sufficient to facilitate or interrupt CT. DNA CT is attenuated by large and small perturbations in π -stacking. Single base mismatches, base modifications and lesions, and even protein binding events that kink the DNA duplex or flip out a base are sufficient to interrupt DNA CT (Boal and Barton, 2005; Gorodetsky et al., 2008a; Hall and Barton, 1997; Kelley et al., 1997a, 1999). Interestingly, nicks in the phosphate-deoxyribose backbone are tolerated as long as the sugar-backbone modifications do not interfere with base-base stacking (Liu and Barton, 2005). DNA CT thus reports on the integrity of the base pair stack.

Our laboratory has focused on studies of DNA charge transport (CT), beginning with understanding the basic chemistry and the parameters that govern charge transport, and moving towards understanding how this chemistry may be harnessed within the cell. Here, we describe that evolution. DNA CT represents powerful chemistry that permits redox reactions to be activated over long molecular distances, enabling sensing of small perturbations to the DNA base pair stack with high sensitivity, and potentially providing a means to communicate across the genome.

Platforms for Exploring DNA Charge Transport

Various platforms for investigating DNA CT have been developed. Two of the most effective platforms consist of photoinduced reactions using DNA assemblies in solution with tethered donors and/or acceptors (Figure 2) and ground state electrochemistry on DNA monolayers (Figure 3). With these very different platforms, the important aspects of DNA CT chemistry are evident: (i) that DNA CT can proceed over long molecular distances; (ii) that DNA CT is sensitive to intervening perturbations in π -stacking.

Photoinduced DNA CT with tethered intercalators

For photoinduced CT experiments in solution, we have utilized DNA assemblies with tethered photooxidants containing an intercalating ligand that allows for π -stacking and thus electronic coupling between the photooxidant and the DNA bases (Figure 2). Irradiation of the photooxidant typically produces an excited state that is sufficiently oxidizing and long-lived to withdraw an electron from DNA. Examples of metallointercalators that have been used to probe the redox properties of DNA include $[\text{Rh}(\text{phi})_2(\text{bpy}')]^{3+}$, $[\text{Ru}(\text{phen})(\text{bpy}')(\text{dppz})]^{2+}$, $[\text{Re}(\text{CO})_3(\text{dppz})(\text{py}')]^+$, and $[\text{Ir}(\text{ppy})_2(\text{dppz}')]^+$, where phi = 9,10-phenanthrenequinone diimine, bpy' = 4-methyl-4'-(butyric acid)-2,2'-bipyridine, phen = 1,10-phenanthroline, dppz = dipyrido[2,3-a:2',3'-c]phenazine, py' = 3-(pyridin-4-yl)propanoic acid, ppy = 2-phenylpyridine, and dppz' = 6-(dipyrido[3,2-a:2',3'-c]phenazin-11-yl)hex-5-ynoic acid (Olmon et al., 2011; Shao and Barton, 2007; Williams et al., 2004). The yield of oxidative DNA damage produced by metallointercalators has been found to depend primarily on the thermodynamic driving force for CT, the efficiency of back electron

transfer (ET) processes, and, importantly, the degree of electronic coupling to the DNA π -stack (Olmon et al., 2011). These complexes can be covalently tethered to DNA by utilizing modified ligands (dppz', bpy', phen') in order to localize the complex to one end of the DNA (Holmlin et al., 1999).

An early example of the application of metallointercalators to the study of DNA CT employed an intercalating donor, a dppz complex of Ru(II), and as acceptor, a phi complex of Rh(III), both of which were tethered to either ends of the DNA duplex (Murphy et al., 1993). The dppz complex is a DNA light-switch: whereas its luminescence is quenched in aqueous solution, upon the addition of DNA, the ruthenium complex luminesces brightly (Friedman et al., 1990). However, when $[\text{Rh}(\text{phi})_2(\text{phen}')^{3+}]$ is appended to the opposite strand, the DNA-bound $[\text{Ru}(\text{phen}')_2(\text{dppz})^{2+}]$ luminescence is completely quenched (Murphy et al., 1993). Nanosecond time-resolved luminescence experiments were too slow to observe this quenching process. Extensive control experiments, including those that ruled out intermolecular events, coupled with the improbability of energy transfer, confirmed that this quenching is due to rapid intramolecular DNA-mediated electron transfer between the metal complexes, from the $^*\text{Ru}^{2+}$ excited state to the rhodium complex. This experiment provided the first insights into long-range DNA charge transport.

Oxidative DNA damage through DNA CT

Besides examining DNA CT spectroscopically, we also used DNA-bound photooxidants to explore oxidative damage to the DNA from a distance using biochemical methods. Here the electron donor was the DNA itself, specifically the 5'-G of guanine doublets and triplets. Because guanine is the most easily oxidized of the DNA bases (Fukuzumi et al., 2005) and the presence of adjacent guanines further lowers the guanine oxidation potential (Sugiyama and Saito, 1996), guanine doublets and triplets are electron hole sinks within DNA. Work in our laboratory demonstrated that oxidative damage can be generated from a distance via DNA CT, and that this damage is localized to these low potential guanine multiplets (Arkin et al., 1997; Hall et al., 1996). Here metallointercalating photooxidants were covalently tethered to one end of the DNA duplex, ensuring spatial separation between the photooxidant and the guanine doublet. After irradiation and piperidine treatment of radiolabeled DNA, damage was observed predominantly at the 5'-G of a guanine doublet located far from the site of metallointercalation. Because the timescale of DNA CT is much faster than the formation of permanent oxidative lesions (*vide infra*), the injected electron hole can equilibrate along the base-pair π -stack and localize to the low potential guanine doublet. Thus the pattern of oxidative damage to guanine multiplets is a characteristic of damage from a distance via DNA CT. In these studies we also observed the sensitivity of DNA CT to intervening perturbations in base pair stacking; introduction of an intervening DNA bulge could turn off the long-range damage (Hall and Barton, 1997). These studies further illustrated the long distances over which DNA CT could proceed: long range oxidative damage to DNA was demonstrated over 200 Å away from the tethered photooxidant, a remarkable molecular distance (Núñez et al., 1999).

The ability to carry out long range oxidative damage is not special to the metallointercalating photooxidants; indeed long range photooxidation of DNA was also

demonstrated using a tethered and helix-capping anthraquinone (Schuster, 2000). Studies with various organic photooxidants underscored how long range oxidative damage depended not on the probe but on the DNA duplex.

Kinetics of DNA CT

Experiments using picosecond spectroscopy explored electron transfer between non-covalently bound, intercalated ruthenium and rhodium metal complexes to learn more about the timescale for DNA CT (Arkin et al., 1996). While even on the picosecond timescale, DNA-mediated CT between the metal complexes was faster than the instrumental resolution; these studies established a lower limit for the electron transfer rate of $3 \times 10^{10} \text{ s}^{-1}$ (Arkin et al., 1996).

The rates of DNA CT along with effects of driving force were then extensively studied on a fast timescale using synthetic DNA hairpins (Lewis et al., 2000). Here mechanistic studies were carried out (see below) and the reorganization energy within the DNA duplex could be determined, but given the rigidity of the crosslinked hairpins, dynamical motions within the duplex are limited, and new tethered probes were required to probe the importance of DNA dynamics to DNA CT.

Femtosecond transient absorption experiments were then able to observe DNA-mediated electron transfer between photoexcited tethered ethidium and a modified base in DNA (Wan et al., 1999). Here, the modified base 7-deazaguanine was positioned at varying distances from the tethered ethidium, which is sufficiently oxidizing in the excited state to oxidize 7-deazaguanine but not the other DNA bases. After femtosecond-resolved laser excitation of the ethidium, 5 ps and 75 ps decay components were observed that can be ascribed to electron transfer from 7-deazaguanine to the ethidium excited state. These two electron transfer rates correspond to different ethidium orientations: the 5 ps rate corresponds to an ethidium orientation that is favorable for CT, whereas the slower 75 ps rate corresponds to an initially unfavorable conformation that requires reorientation or rotation of the ethidium in order for CT to occur (Wan et al., 1999). Importantly, the rates of electron transfer are unaffected by donor-acceptor distance from 10 to 17 Å. However, the efficiency of CT was observed to decrease with increasing distance. Hence it appears that the CT is gated by the motions of the base pairs. Overall, this study demonstrated the ultrafast nature of favorable electron transfer through DNA, as well as the shallow distance dependence of the CT rate and the importance of DNA dynamics. Interestingly, in another study where the ethidium was incorporated into the DNA in a more constrained conformation, no CT could be observed; these subtle changes reflect the sensitivity of DNA CT to stacking dynamics and electronic coupling (Valis et al., 2006).

DNA Electrochemistry

In addition to DNA photooxidant assemblies in solution, the other major platform that has been effectively used to study DNA CT in our laboratory has been electrochemistry on DNA monolayers (Figure 3). Here we can explore DNA CT in the ground state. Typically, a single strand of DNA is modified with a terminal alkanethiol moiety and annealed to its complementary strand. These thiol-modified DNA duplexes can then be self-assembled into

DNA monolayers on gold electrode surfaces, forming covalent gold-thiol bonds (Kelley et al., 1997b). Monolayers can be assembled in the absence and presence of MgCl_2 to create low and high density monolayers, respectively (Pheeny and Barton, 2012). More recently, click chemistry methods have been utilized to enable controlled variation in the amount of DNA on the surface, while concurrently producing more evenly spaced monolayers (Furst et al., 2013). Finally, DNA can also be functionalized with pyrene to form DNA monolayers on highly oriented pyrolytic graphite (HOPG), allowing for a wider potential window than gold electrodes (Gorodetsky and Barton, 2006).

After DNA monolayer formation, a DNA-bound redox probe can be exploited to investigate DNA CT on a surface. Organic dyes such as Nile blue and methylene blue have been commonly used as redox probes (Kelley et al., 1997b; Pheeny and Barton, 2012; Slinker et al., 2011). In these systems, charge can flow directly from the electrode to the redox probe, or charge can be conducted in a DNA-mediated fashion, flowing from the electrode through the alkane-thiol tether and the DNA π -stack to reach the redox probe. Here again, stacking of the redox probe with the DNA base-pair π -stack to facilitate electronic coupling is vital (Boon et al., 2003a). The intercalated redox probe may be covalently tethered to the distal end of the DNA relative to the electrode surface; in this case, the nature of the linkage to the DNA is also important (Gorodetsky et al., 2007). Long, saturated linkages do not maintain electronic coupling to the DNA π -stack and thus do not facilitate DNA CT, in contrast to short, unsaturated linkages which preserve this coupling (Gorodetsky et al., 2007).

A DNA-mediated pathway can be demonstrated by comparing well-matched DNA with DNA that contains a mismatch or abasic site; the disruption to the base pair π -stacking attenuates the amount of charge that reaches the redox probe (Figure 3). Electrochemical charge transport through the DNA π -stack can occur well below the potential of individual DNA bases, likely due to charge delocalization (Genereux and Barton, 2010). Therefore, unlike experiments with DNA photooxidants, these experiments do not involve potentials that damage the DNA. Instead, at these potentials CT is much like that through graphite (in the perpendicular direction to the graphene sheets), where charge migration depends upon a delocalized interaction among the π -stacked sheets. Indeed, using single molecule electrochemical studies, where we measured DNA CT across a carbon nanotube gap, we found the resistivity of the DNA duplex to be quite close to that calculated for a segment of graphite of similar size arranged in the perpendicular direction in the nanotube gap (Guo et al., 2008). Again in this experiment, the presence of a single base mismatch interfered with CT and increased the resistivity of the DNA duplex 100-fold.

DNA electrochemistry experiments have directly demonstrated the shallow distance dependence of DNA CT (Slinker et al., 2011). Multiplexed chips were developed that allow for simultaneous investigation of up to four different types of DNA on a single gold surface with four-fold redundancy (Slinker et al., 2010). An application of these chips directly compared DNA CT between 17-mer and 100-mer duplexes covalently modified on the distal end with a Nile blue redox probe (Slinker et al., 2011). In quadrants of the multiplexed chip where a single C:A mismatch was incorporated into the 100-mer duplex, DNA CT was significantly attenuated even over this long molecular distance, indeed to the same extent as for the 17-mer. Moreover, the estimated ET rates of $25 - 40 \text{ s}^{-1}$ were indistinguishable

between the 17-mer and 100-mer duplex constructs, indicating that tunneling through the alkanethiol tether is still rate-limiting, consistent with earlier work (Drummond et al., 2004), while CT through the DNA 100-mer is rapid. Overall, this DNA electrochemistry experiment established that charge is efficiently transported through DNA in the ground state over long molecular distances, at least up to 100 base pairs or 34 nm, the longest documented distance for this type of molecular wire.

Mechanism of DNA CT

Many experiments taken together suggest a model for the mechanism of DNA CT, although there is much we still need to understand. Superexchange involves coherent orbital-mediated tunneling along the entire DNA bridge between the electron donor and acceptor and displays an exponential dependence of the rate of electron transfer on distance. This substantial distance dependence with a superexchange mechanism is inconsistent with the fast electron transfer rates that have been measured over relatively long molecular distances (Genereux and Barton, 2010). For example, the DNA-mediated electron transfer from excited $[\text{Ru}(\text{phen}')(\text{dppz})]^{2+}$ to $[\text{Rh}(\text{phen})_2(\text{phen}')]^{3+}$ occurs over a distance of 41 Å within just 3 nanoseconds (Murphy et al., 1993).

Instead, an incoherent hopping mechanism, where there is some intermediate state of charge localization on the bridge, is more likely for long-range charge transport through DNA because of its more shallow distance dependence. One hopping proposal consists of thermally induced localized hopping on individual DNA bases (Giese et al., 2001). Localized hole hopping is typically envisioned as occurring through guanine hopping, given that guanine is the most easily oxidized base (Fukuzumi et al., 2005, Berlin et al., 2001), but this mechanism does not explain several experimental observations regarding DNA CT, such the coherent transmission of the energy of the injected charge to the final distal acceptor or the ground state electrochemical studies (Genereux and Barton, 2010). Alternatively, a delocalized hopping mechanism is possible wherein charge is delocalized over multiple bases. Based on studies with the photooxidant anthraquinone, Schuster and coworkers proposed that such delocalization could occur through a thermally assisted polaron hopping mechanism (Schuster, 2000). However, thermal activation mechanisms still do not explain ground state electrochemistry studies where transport occurs significantly below the potentials of the DNA bases (Kelley et al., 1997b). Overall, many researchers have now found evidence for charge delocalization along multiple DNA bases during DNA CT (Kawai and Majima, 2013; Renaud et al., 2013; Genereux et al., 2011).

Importantly, a periodic oscillation with distance has been observed in different systems measuring DNA CT. Work by Tao and coworkers investigated the resistance of duplexed DNA between two electrodes (Xiang et al., 2015). They found that the resistance of the DNA circuit, which is inversely proportional to CT rate, increases linearly with distance, and detected an oscillation with a period of 2 to 3 bases in sequences with stacked GC base-pairs (Xiang et al., 2015). Similarly, in photooxidation experiments, our group has observed a periodic oscillation of the yield of DNA CT with distance with a period of 3 to 4 bases (O'Neill and Barton, 2004; Genereux et al., 2008). The source of this oscillation is

considered as the delocalization of electrons or electron holes along the number of DNA bases in the period and depends sensitively on the sequence-dependent dynamics of DNA.

Taken together, current experimental evidence suggests that charge transport through DNA is best described as a partially coherent hopping mechanism, consisting of multiple hopping steps between delocalized (approximately 3 base pair) domains of well-coupled stacked bases (O'Neill and Barton, 2004; Xiang et al., 2015). These CT-active domains of π -stacked bases are created through conformational dynamics of the bases that modulate their electronic coupling. Coherent superexchange would occur along these π -stacked domains of approximately 3 base pairs. Thus DNA CT can essentially be envisioned as hopping between adjacent stacked regions in the DNA. This mechanism also explains why a mismatch or lesion would attenuate DNA CT: it perturbs the formation of these well-coupled 3 base pair delocalized domains, and does so similarly in long and short DNA duplexes.

Detection and diagnostic applications of DNA CT

Given the sensitivity of DNA CT to structural modifications that disrupt π -stacking of the bases, DNA-modified electrochemistry can be harnessed for the detection of DNA damage, base modifications, and DNA-binding proteins that either attenuate CT or contain redox-active moieties that couple into the DNA π -stack. DNA-modified electrodes that employ DNA CT as a reporting mechanism have been used to detect single base mismatches (Boon et al., 2000; Kelley et al., 1999; Slinker et al., 2010) and a variety of DNA lesions such as oxidized bases (Boal and Barton, 2005), all of which disrupt the dynamics of base-pair stacking within DNA (Genereux and Barton, 2010). Additionally, proteins that disrupt the structure of DNA can be effectively detected. These proteins include enzymes that flip bases out of the helix during enzymatic activity such as the HhaI methylase or uracil DNA glycosylase (Boon et al., 2002). The TATA-binding protein can also be detected electrochemically using DNA CT because it significantly kinks the DNA when bound (Boon et al., 2002; Furst et al., 2013; Gorodetsky et al., 2008a).

DNA CT methods can measure not only the presence but also the activity of DNA-processing enzymes. One such example is detection of human methyltransferases activity. It is well established that hyper- and hypo-methylation within cells is an early marker of numerous cancerous phenotypes (Baylin and Herman, 2000; Das and Singal, 2004) and that the methylation levels are correlated with the levels of methyltransferase activity. Unfortunately, currently available methods to detect methyltransferase activity in the clinic are comparatively expensive, time-consuming, and are not as sensitive. In contrast, the activity of human methyltransferases can be sensitively detected using DNA-modified electrodes (Figure 4). Within this assay, DNA-modified electrodes containing a hemimethylated DNA substrate are incubated with Dnmt1, a methyltransferase that prefers to methylate hemimethylated DNA. Next, the electrodes are treated with a restriction enzyme that preferentially cuts unmethylated or hemimethylated DNA. Fully methylated DNA, which arises from methylation by Dnmt1, is protected from restriction enzyme cutting (Muren and Barton, 2013). Given that the electrochemical readout is provided by a redox-active probe intercalated into DNA on the surface of the electrode, signal attenuation occurs

if the unmethylated or hemi-methylated DNA is cut by the restriction enzyme and the probe is released into solution. Thus, the retention of the electrochemical current following treatment with the restriction enzyme represents a signal-on reporter of the activity of the methyltransferase. The methylation activity of human Dnmt1 has been detected using this electrochemical strategy in a variety of contexts and coupled to electrocatalysis in a two-electrode platform for high sensitivity in detection (Furst and Barton, 2015; Furst et al., 2014; Muren and Barton, 2013).

Most recently, DNA-modified electrodes have been used to detect Dnmt1 from the crude lysates of tumor samples, eliminating the need to purify the tumor sample prior to analysis (Furst et al., 2014). By electrochemically measuring the activity of Dnmt1 using these DNA-modified electrodes, hyperactivity of Dnmt1 in colorectal cancer tumors but not adjacent tissue is observed. Notably, this hyperactivity cannot be observed by assaying for Dnmt1 expression using qPCR or western blotting, which measure protein amount rather than activity, nor by assaying activity using a much less sensitive radiometric labeling assay (Furst and Barton, 2015). This strategy can be expanded to encompass different families of DNA-binding proteins and thus offers a completely new platform for rapid and sensitive detection and diagnosis in cell lysates.

We can also use these DNA electrodes to monitor the redox cofactors inherently present in many DNA processing enzymes. MutY, a base excision repair (BER) protein containing a [4Fe4S] cluster, was the first protein to be thus investigated (Boon et al., 2003b). Importantly, these studies were able to determine the *DNA-bound* redox potential of MutY. The observed redox potential of 90 mV versus NHE was assigned to the [4Fe4S]^{3+/2+} couple, and is consistent with potential ranges for high potential iron-sulfur proteins (HiPIPs). The DNA-mediated nature of the electrochemical signal was confirmed through introduction of an intervening abasic site in the DNA that attenuated the signal. Finally, a MutY mutant was assayed wherein one of the ligating cysteine residues of the [4Fe4S] cluster was changed to a histidine; C199H MutY displayed a redox potential of 65 mV versus NHE, a negative shift relative to the WT protein as expected for histidine ligation (Boon et al., 2003b). This mutant experiment confirmed the iron-sulfur cluster as the origin of the observed electrochemical signal. Indeed, an array of DNA-processing enzymes containing iron-sulfur clusters have now been detected using DNA-modified electrochemistry (Grodick et al., 2015).

DNA CT by Repair Proteins containing [4Fe4S] Clusters

How might DNA charge transport be used by proteins inside the cell? Following the work with *E. coli* MutY (Boon et al., 2003b), other BER proteins with [4Fe4S] clusters were discovered to have similar DNA-bound [4Fe4S]^{3+/2+} reduction potentials, including *E. coli* Endonuclease III (EndoIII) and *Archeoglobus fulgidus* uracil DNA glycosylase (UDG) (Boal et al., 2005). As the first step in the BER pathway, these glycosylase enzymes prevent mutagenesis by, for example, removing adenine mispaired with 8-oxoguanine in the case of MutY, or oxidized pyrimidines in the case of EndoIII, followed by the insertion of the correct base by a polymerase (Kim and Wilson, 2012). While the mechanistic details of glycosylase enzymes once they have found their substrates are relatively well understood

(David et al., 2007), how the search is efficiently coordinated is less clear given their low copy numbers in the cell. In *E. coli*, there are an estimated 500 copies of EndoIII per cell, and only approximately 30 copies of MutY (Demple and Harrison, 1994). Given their low copy numbers and the vast quantity of DNA that must be searched, diffusion-only search models simply are too slow to permit scanning of the entire genome within the doubling time of *E. coli* (Boal et al., 2009).

Could the [4Fe4S] cluster of these glycosylase enzymes be involved in the search process? The [4Fe4S]²⁺ cluster of EndoIII is relatively insensitive to reduction and oxidation in solution (Cunningham et al., 1989), leading originally to a proposed structural role for the cluster, although it is not required for folding or stability in the homologous enzyme MutY (Porello et al., 1998). However early redox studies of these proteins were performed in the absence of the DNA polyanion, which surely could be expected to alter the cluster potential. Using DNA-modified electrodes, we measured the DNA-bound potential of these proteins and found that the redox potential of the EndoIII cluster shifts upon DNA binding (Gorodetsky et al., 2006). On DNA-modified HOPG electrodes, the observed midpoint potential of 20 mV versus NHE was assigned to the [4Fe4S]^{3+/2+} couple, similarly to what had been previously reported on DNA-modified gold electrodes. On bare HOPG, without DNA, two signals were observed: an irreversible anodic peak at 250 mV and a cathodic peak at -300 mV, assigned to the [4Fe4S]^{3+/2+} and [4Fe4S]^{2+/1+} couples, respectively. Thus DNA binding negatively shifts the [4Fe4S]^{3+/2+} redox potential of the cluster by at least 200 mV, activating the cluster towards oxidation (Gorodetsky et al., 2006). Because significant conformational changes do not occur upon DNA binding, a thermodynamic consequence of this shift in redox potential is that the oxidized [4Fe4S]³⁺ form of EndoIII has a much higher affinity for DNA (3 orders of magnitude) than the reduced [4Fe4S]²⁺ form. Lower DNA binding affinity for the reduced enzyme was also observed qualitatively with bulk electrolysis experiments on EndoIII, MutY, and UDG (Boal et al., 2005). Therefore while these proteins are relatively insensitive to oxidation in solution, the redox potential of the [4Fe4S] cluster shifts into the physiologically relevant range when bound to DNA.

The combination of (i) the negative shift in redox potential of the [4Fe4S] cluster of glycosylase enzymes upon DNA binding that entails higher binding affinity in the oxidized [4Fe4S]³⁺ state compared to the reduced [4Fe4S]²⁺ state, (ii) similar DNA-bound [4Fe4S]^{3+/2+} redox potentials of approximately 80 mV versus NHE for all of the enzymes studied, and (iii) the rapid kinetics of DNA CT (ps), suggested a model whereby these proteins could use interprotein DNA-mediated CT, in a kind of electron transfer self-exchange reaction, to cooperate in order to find lesions inside the cell (Boal et al., 2009) (Figure 5). In this model, a repair enzyme containing a [4Fe4S] cluster, bound to DNA in the reduced form, could initially become oxidized through DNA CT by guanine radicals in DNA or reactive oxygen species. A second enzyme, also containing a [4Fe4S] cluster, binds DNA within (at a minimum) 100 bases of the first enzyme, becoming activated towards oxidation and releasing an electron into the π -stack of the DNA. This electron can then reduce the first distally bound repair enzyme via DNA CT if the intervening DNA is undamaged, resulting in dissociation of this reduced enzyme. The repair proteins have thus scanned this intervening region of the genome and found it to be free of damage. Because

the DNA-bound redox potentials of the clusters are very similar, this interprotein DNA-mediated CT can be viewed as an activationless self-exchange CT reaction. However, if there is a lesion in the DNA between the proteins, DNA CT will be attenuated and the electron will not efficiently reach the distal protein. Instead, both proteins will remain bound to the DNA and can processively diffuse to the location of damage. In this manner, the range over which the slower process of diffusion must occur is significantly reduced. Thus we propose that DNA-mediated signaling would be an efficient way to localize BER proteins to the vicinity of DNA lesions within the cell.

Observing protein redox activation via DNA CT spectroscopically

Experiments first focused on gathering *in vitro* evidence for the feasibility of [4Fe4S] cluster oxidation in proteins by guanine radicals through DNA CT. MutY oxidation via the flash-quench technique was monitored by EPR and transient absorption spectroscopies (Yavin et al., 2005). After the “flash” of photoinduced excitation, the Ru²⁺ photooxidant excited state is oxidatively “quenched” by a diffusing molecule in order to yield a highly oxidizing intercalated ground state Ru³⁺ species *in situ*. With DNA, [Ru(phen)₂(dppz)]²⁺, a diffusing quencher, and MutY, *g*-values consistent with the oxidation of the cluster to [4Fe4S]³⁺ and its decomposition product, the [3Fe4S]⁺ cluster, are observed upon irradiation using low temperature EPR. With similarly composed transient absorption experiments utilizing alternating poly(dG-dC) DNA, a very long-lived positive transient is observed with a fast phase corresponding to guanine radical and a slow phase with characteristics consistent with [4Fe4S]³⁺, also indicating oxidized MutY. Importantly, the long-lived positive transient is not observed with poly(dA-dT), suggesting the importance of guanine radical as an intermediate in DNA CT to yield MutY oxidation. Furthermore, the yield of guanine oxidation was monitored biochemically in radiolabeled mixed sequence DNA containing a guanine doublet (Yavin et al., 2005). In the absence of MutY, damage is localized specifically to the 5'-G of the guanine doublet as expected for oxidative damage generated through DNA CT; this damage is inhibited upon titration with MutY. Overall, these data indicate that while MutY can be oxidized without guanine radical as an intermediate, the thermodynamically favorable oxidation of the MutY [4Fe4S]²⁺ cluster by guanine radical enables more efficient MutY oxidation.

Subsequently, EPR experiments with a nitroxide spin label conjugated to uracil within the DNA sequence demonstrated the feasibility of CT from both EndoIII and MutY to the oxidized spin label (Yavin et al., 2006). The EPR-active, *S* = ½ nitroxide species can be oxidized with a mild Ir⁴⁺ oxidant to yield an EPR-silent species with a reduction potential sufficient to oxidize the [4Fe4S]²⁺ cluster of BER proteins. The reappearance of the nitroxide signal upon the addition of protein indicates iron-sulfur cluster oxidation to reduce the spin label. A DNA-mediated mechanism is suggested because of the dependence of spin probe reduction on the electronic coupling of the nitroxide spin label: when the spin label is well-coupled to the DNA via an unsaturated linkage, the nitroxide is efficiently reduced, whereas the reduction yield is significantly attenuated with a poorly coupled saturated linkage. The spin label thus acts as a trap for DNA-mediated CT from the proteins.

DNA CT within the cell

In eukaryotic cells, genomic DNA is not freely accessible but is instead wrapped around histones to form nucleosome core particles. To answer the question of whether DNA CT is feasible under cellular conditions, we investigated oxidative DNA damage induced by tethered $[\text{Rh}(\phi)_2(\text{bpy}')^3]^+$ in DNA with and without bound histones (Núñez et al., 2002). The level of damage to a distal guanine doublet was nearly identical between bare DNA and histone-wrapped DNA, indicating that DNA CT is not attenuated in nucleosome core particles. Although DNA may be protected from some damage when packaged into nucleosomes, it is not protected from damage created through DNA CT as electron holes flow freely through histone-wrapped DNA.

Furthermore, there is significant protein traffic on DNA in living cells, including transcription factors and DNA processing enzymes. While DNA CT is attenuated by proteins that distort DNA π -stacking by significantly bending the DNA (i.e., TATA binding protein) or flipping out a DNA base, DNA CT is preserved amidst protein traffic that maintains DNA π -stacking (Gorodetsky et al., 2008a; Rajski and Barton, 2001). In fact, DNA CT can even be slightly enhanced by protein binding, potentially due to the rigidifying effect of protein binding on base stacking. Hence DNA CT can occur in nucleosome core particles and is tolerant of most protein traffic, making it feasible *in vivo*.

Inter-Protein Signaling through DNA CT

Signaling between base excision repair proteins

Subsequent work in our laboratory focused on garnering both *in vitro* and *in vivo* evidence for interprotein signaling via DNA CT. Our model predicts a redistribution of BER proteins from regions of undamaged DNA to the vicinity of a lesion (Figure 5). Using atomic force microscopy (AFM), we have shown that WT EndoIII does indeed redistribute from short well-matched DNA strands onto long strands containing a lesion (Boal et al., 2009). The lesion we utilized was a single C:A mismatch which inhibits DNA CT but is not itself a substrate for EndoIII. Redistribution is quantified as a binding density ratio, r , of the number of proteins on the long mismatched strands relative to those on short matched strands; a binding density ratio of 1 would indicate equal protein distribution. For WT EndoIII, a binding density ratio of 1.6 ± 0.1 is observed that is even more pronounced in the presence of increasing concentrations of hydrogen peroxide. According to our model, some level of protein oxidation is necessary for redistribution; redistribution is enhanced under conditions that simulate oxidative stress in the cell. The redistribution is also found to be dependent on the proficiency of the protein for DNA CT. For example, mutation of an aromatic tyrosine residue to an alanine (Y82A) results in a protein that is electrochemically deficient in DNA CT but proficient in enzymatic glycosylase activity (Boal et al., 2009) (Figure 6). Likely because of poorer electronic coupling, less charge can be passed to the [4Fe4S] cluster, resulting in a lower signal intensity in cyclic voltammetry experiments. Importantly, Y82A EndoIII is unable to redistribute onto mismatched strands in the AFM assay because of its inability to perform effective DNA CT. Indeed we have seen that the binding density ratio correlates directly with the efficiency of DNA-mediated CT (Romano et al. 2011); the

greater the efficiency of DNA-mediated CT by an EndoIII mutant, the greater the propensity to find the mismatched strand, and the higher the resulting binding density ratio.

We have also utilized a genetic assay measuring the cooperativity of BER proteins through signaling *in vivo* (Boal et al., 2009). A *lac*⁺ reversion assay within the CC104 strain of *E. coli* can be used to quantify MutY activity; thus, a gene of interest can be knocked out to investigate the resultant effects on MutY activity inside living cells. When the gene for EndoIII is knocked out, *lac*⁺ revertants increase reflecting a decrease in MutY activity although MutY and EndoIII target different lesions within the cell, indicating that EndoIII contributes to MutY activity by some other mechanism. DNA-mediated signaling between EndoIII and MutY to assist the very low copy number MutY to localize to the vicinity of lesions is suggested by experiments with EndoIII mutants. Restoring CT-deficient Y82A EndoIII to the *E. coli* strain does not rescue MutY activity. Conversely, D138A EndoIII, while deficient in glycosylase activity, retains an intact 4Fe4S cluster and the ability to transport charge, and is able to rescue MutY activity. Consequently, the important factor for EndoIII rescuing MutY activity is proficiency for DNA CT. This assay was the first indication of inter-protein DNA CT within cells.

Importantly, our model for redistribution would provide a feasible means for proteins to locate lesions within the time constraints imposed by replication, and since CT would occur through the base π -stack, the process can bypass protein traffic. It must be emphasized that a DNA-CT mediated signaling mechanism as a first step for binding within the vicinity of damage is not mutually exclusive with other proposed models of DNA damage recognition by glycosylases and, in fact, could complement existing strategies (Blainey et al., 2006; Friedman and Stivers, 2010; Fromme et al., 2004; Wallace, 2013).

Signaling between distinct repair pathways: nucleotide excision repair helicase, XPD

Other DNA repair proteins outside the BER pathway have been found with similar DNA-bound [4Fe4S]^{3+/2+} redox potentials. XPD is an ATP-dependent nucleotide excision repair (NER) helicase with a 4Fe4S cluster. On DNA-modified electrodes, archaeal XPD from the thermophile *Sulfolobus acidocaldarius* (SaXPD), was found to have a DNA-bound potential of 80 mV versus NHE that is sensitive to an intervening mismatch (Mui et al., 2011). Interestingly, an increase in the electrochemical signal intensity is observed upon the addition of ATP to SaXPD on the DNA-modified electrode surface but is not observed in the presence of the slowly hydrolyzable analog ATP- γ -S. An ATPase and helicase deficient mutant, G34R XPD, also does not display this increase in current. Therefore the signal increase upon ATP addition was ascribed to conformational changes associated with ATP hydrolysis, demonstrating that DNA-mediated electrochemistry can report on enzymatic activity.

AFM studies combining EndoIII and XPD give direct *in vitro* evidence for inter-protein DNA-mediated signaling (Sontz et al., 2012). Initial AFM studies showed that WT XPD redistributes from short matched DNA strands to long mismatched strands with a binding density ratio similar to that of WT EndoIII. In contrast, L325V XPD, an electrochemically CT-deficient XPD mutant, does not redistribute, analogously to Y82A EndoIII. Equimolar mixtures of XPD and EndoIII were then assayed at concentrations where approximately 2

proteins are bound per DNA strand. Remarkably, mixtures of the *E. coli* BER protein EndoIII and archaeal NER protein XPD efficiently redistribute, localizing to the vicinity of a DNA lesion (Sontz et al., 2012). However, this redistribution is not observed if either protein in the mixture is CT-deficient, likely because, at these protein loadings, a CT-deficient protein results in no partner for the electron transfer self-exchange reaction. When WT XPD is titrated into Y82A EndoIII at a ratio of 3:1, efficient redistribution is recovered because there is a significant population of partners of CT-proficient proteins. Therefore, given similar DNA-bound redox potentials of their $[4\text{Fe}4\text{S}]^{3+/2+}$ clusters, proteins from different repair pathways, in fact even different organisms, can use DNA-mediated CT to cooperate in order to find lesions.

Signaling between distinct repair pathways in vivo

DinG is an *E. coli* DNA damage-inducible helicase with a $[4\text{Fe}4\text{S}]$ cluster and homology to XPD as well as to other eukaryotic helicases. DinG performs the vital function of unwinding RNA-DNA hybrid structures, called R-loops, which result from stalled replication forks (Boubakri et al., 2010; Ren et al., 2009; Voloshin et al., 2003). When investigated on DNA-modified electrodes, DinG displays a DNA-bound redox potential of 80 mV versus NHE (Grodick et al., 2014), the same DNA-bound $[4\text{Fe}4\text{S}]^{3+/2+}$ potential that had been observed for the BER proteins and SaXPD (Boal et al., 2005; Mui et al., 2011). Like the fellow ATP-dependent helicase XPD, the intensity of the DinG electrochemical signal increases upon ATP addition. Utilization of the AFM assay demonstrated *in vitro* redistribution with solely WT DinG proteins as well as with equimolar mixtures of WT DinG and EndoIII proteins; conversely, redistribution does not occur in a 1:1 mixture of WT DinG with Y82A EndoIII.

We also used genetic assays to test for signaling within the cell. A modest decrease in MutY activity *in vivo* upon knocking out DinG is observed in the CC104 *lac*⁺ reversion assay. This defect can be rescued by complementing the cells with a plasmid that constitutively expresses D138A EndoIII but not Y82A EndoIII, suggesting DNA-mediated cross-talk between MutY, DinG, and EndoIII inside cells (Grodick et al., 2014).

A much more dramatic *in vivo* result was found with the InvA strain of *E. coli* (Figure 7). By inverting a highly transcribed ribosomal RNA operon, the InvA strain contains an increased frequency of collisions between the transcriptional and replication machineries, forming stalled replication forks (Boubakri et al., 2010). The resulting RNA-DNA hybrid structures must be unwound by DinG to maintain cellular viability. Signaling between DinG and EndoIII was investigated *in vivo* by knocking out the gene for EndoIII within the InvA *E. coli* strain. Bacterial growth is severely impaired in this InvA EndoIII knockout strain. An R-loop phenotype was implicated by rescue with RNaseH, as this enzyme selectively degrades RNA in RNA-DNA hybrids. Bacterial growth could also be restored by complementation with WT or D138A EndoIII, but not Y82A EndoIII, indicating that EndoIII and DinG cooperate via a DNA-mediated CT mechanism (Grodick et al., 2014). This result provides compelling *in vivo* evidence for DNA CT between DinG and EndoIII to assist DinG in maintaining cellular viability under the adverse conditions caused by increased collisions between the transcriptional and replication machineries.

The number of DNA processing enzymes shown to contain [4Fe4S] clusters continues to increase. For example, in addition to glycosylase and helicase enzymes involved in DNA repair, [4Fe4S] clusters have been found in RNA polymerase (Hirata et al., 2008), all four yeast B-family DNA polymerases (Netz et al., 2012), as well as in primase (Weiner et al., 2007). As more potential electron self-exchange partners are discovered, DNA-mediated signaling becomes an increasingly viable mechanism that could be utilized to coordinate not only DNA repair, but also transcription and replication in organisms from bacteria to man (Fuss et al., 2015).

DNA CT in Response to Oxidative Stress

SoxR, a transcriptional sensor

DNA charge transport may also be used biologically to promote cellular responses to oxidative stress both in bacteria and eukaryotes for the long-range and selective activation of redox-active transcription factors (Figure 8). SoxR is a homodimeric bacterial transcription factor that responds to superoxide stress, containing a [2Fe2S]^{2+/+} cluster within each monomer (Watanabe et al., 2008). In *E. coli*, oxidation of the [2Fe2S] cluster of SoxR causes a conformational change which improves an RNA polymerase binding site, stimulating transcription of SoxS, a secondary transcription factor, which in turn induces the transcription of about 100 genes to combat superoxide stress (Imlay, 2008). There were many questions regarding the direct oxidant of SoxR *in vivo*. While *in vitro* experiments support direct oxidation of the [2Fe2S] cluster by superoxide (Fujikawa et al., 2012), *in vivo* experiments indicated weak induction by superoxide and instead suggested SoxR oxidation by redox cycling drugs (Gu and Imlay, 2011) or the modulation of cellular NADPH content (Krapp et al., 2011). Adding to the confusion, the measured redox potential of the protein cluster [2Fe2S]^{2+/+} in solution (-290 mV versus NHE) is such that SoxR could be oxidized by many cellular oxidants, even in the absence of oxidative stress.

We considered whether DNA-mediated CT might play a role in SoxR oxidation and more generally in activation of the cellular response to oxidative stress. Using DNA electrochemistry, we found first that DNA binding shifts the redox potential of the [2Fe2S] cluster of SoxR (Gorodetsky et al., 2008b). The positive shift in potential by 500mV to 200 mV versus NHE upon DNA binding means that DNA-bound SoxR is primarily in its transcriptionally inactive, reduced form *in vivo*, solving the conundrum found using the solution potential measured without DNA.

It was then established that SoxR could be activated for transcription *from a distance* through long-range DNA-mediated oxidation (Lee et al., 2009). First, it was demonstrated that reduced SoxR with remaining dithionite, but not oxidized SoxR or dithionite alone, inhibits oxidative damage to a guanine doublet that had been generated via the flash-quench technique. Moreover, SoxR can be activated *in vivo* using the photooxidant [Rh(phi)₂bpy]³⁺, which specifically induces DNA damage via DNA-mediated CT rather than by general production of reactive oxygen species such as would be expected by redox-cycling drugs. *E. coli* cells were treated with [Rh(phi)₂bpy]³⁺, irradiated, and the resulting level of *soxS* mRNA transcript quantified by reverse transcription PCR. Under these conditions, the *soxS* transcript is significantly induced, indicating the feasibility of SoxR activation by DNA

oxidation in cells. Finally, an abortive transcription assay was used to observe directly transcriptional activation from a distance through DNA-mediated oxidation of SoxR. Here, $[\text{Rh}(\text{phi})_2(\text{bpy}')^3]^3+$ was tethered to the 5' end of the DNA, 80 base pairs from the SoxR binding site (Figure 8A). The DNA sequence also contained the promoter binding regions of *soxS*, where upon SoxR oxidation, RNA polymerase will bind and initiate *soxS* transcription. Starting with reduced, transcriptionally inactive SoxR, samples were irradiated, and then incubated with RNA polymerase and ribonucleotides. Remarkably, a 4-mer radiolabeled mRNA corresponding to *soxS* could be detected at significant levels. This activation was triggered simply by irradiation that results in DNA oxidation; furthermore, long-distance electron transfer is ensured by the physical separation of the photooxidant and SoxR.

These results suggested a model for transcriptional activation of SoxR where reactive oxygen species abstract electrons from DNA and electron holes thus produced localize to low potential sites within the DNA, i.e., guanine multiplets. This process results in rapid oxidation of SoxR via DNA CT, filling of the guanine radical hole and activation of transcription (Lee et al., 2009). Transcriptional activation from a distance via DNA CT could thus represent a unifying mechanism for SoxR activation *in vivo*.

Dps proteins, mini-ferritins that bind DNA

We also considered whether DNA CT might play a role in the response of pathogenic bacteria to oxidative stress, an important issue in how host cells respond to pathogenic infection. Dps proteins are bacterial mini-ferritins that are produced in high concentrations in response to stress. These proteins are thought to protect DNA from oxidative stress by utilizing their ferroxidase activity to deplete ferrous iron and hydrogen peroxide, which can otherwise produce damaging hydroxyl radicals via Fenton chemistry (Zeth, 2012). Some Dps proteins also nonspecifically bind DNA, such as that from *E. coli*, which utilizes N-terminal lysine residues for DNA binding (Ceci et al., 2004). Dps is implicated in the survival and virulence of pathogenic bacteria such as *Bacteroides fragilis*, the most common anaerobic species isolated from clinical infections which is both highly aerotolerant and resistant to oxidative stress (Sund et al., 2008), and *Borrelia burgdorferi*, the causative agent of Lyme's disease (Li et al., 2007), among others (Halsey et al., 2004; Olsen et al., 2005; Pang et al., 2012; Satin et al., 2000; Theoret et al., 2012). Fully elucidating the mechanism by which Dps proteins protect pathogenic bacteria from the host immune response could inform the development of new antibiotics.

Previous studies toward revealing the mechanism of Dps protection have shown that Dps protects DNA from DNase cleavage (Almirón et al., 1992), traps hydroxyl radicals, and inhibits DNA nicking by the Fenton reagents Fe^{2+} and H_2O_2 (Zhao et al., 2002). Could the effective protection by ferritins also be derived from using DNA CT to exert protective effects from a distance? Thus, in addition to direct diffusion of oxidants to the iron bound at the ferroxidase sites of Dps, the protein could be envisioned to become oxidized from a distance through DNA CT, thereby protecting the surrounding DNA for potentially hundreds of base pairs.

In order to investigate the possibility of Dps protection from a distance via DNA CT, a tethered ruthenium photooxidant was employed to generate oxidative DNA damage to

mixed sequence DNA via the flash-quench technique, mimicking damage that occurs *in vivo* as a result of oxidative stress (Arnold and Barton, 2013) (Figure 8B). In the absence of protein, oxidative damage localizes specifically to a low potential guanine triplet within the 70-mer duplex, as expected for electron holes equilibrating along the DNA π -stack (Hall et al., 1996). The level of oxidative DNA damage at this guanine triplet can be quantified by using radiolabeled DNA, allowing for analysis of whether Dps can attenuate this guanine damage.

Interestingly, the protective effects of Dps vary as a function of the iron content of the protein (Arnold and Barton, 2013). When no iron is present as in Apo-Dps and or when the ferroxidase sites of the protein are loaded with oxidized ferric iron, which both lack available reducing equivalents, little change in the level of guanine oxidation is observed upon addition of protein. However, when the ferroxidase sites of Dps are loaded with ferrous iron, the yield of oxidative DNA damage at the guanine triplet is significantly attenuated. These data demonstrate that ferrous iron-loaded Dps is selectively oxidized to fill guanine radical holes, thereby restoring the integrity of the DNA. Ruthenium luminescence studies indicate no direct interaction between the photooxidant and Dps, supporting the DNA-mediated oxidation of ferrous iron-loaded Dps. Thus DNA CT may be a mechanism by which Dps proteins efficiently protect the genome of pathogenic bacteria from a distance, contributing to their survival and virulence. Finding methods to disrupt Dps protection from a distance via DNA CT could reveal novel ways to treat bacterial infections.

Protein p53, global regulator of cellular response

While focus has mainly concentrated on proteins that contain metals as their redox-active cofactors, metal clusters are not a requirement for proteins to be able to carry out DNA CT. The tumor suppressor protein p53 is a tetrameric transcription factor that decides cellular fates by selectively binding to different promoter sites within the genome to favor DNA repair and survival or, instead, apoptotic cell death (Vousden and Lu, 2002). But how is that decision rapidly transmitted across the genome? While p53 does not contain an iron-sulfur cluster, there is a network of redox-active cysteine residues whose oxidation state modulates p53 DNA binding. Specifically, p53 oxidation promotes dissociation from the DNA. Given the close proximity of some of these redox-active cysteine residues to the DNA (Cho et al., 1994) and the demonstrated feasibility of disulfide bond formation from a distance via DNA CT (Takada and Barton, 2005), we investigated whether p53 could be oxidized in a DNA-mediated fashion (Augustyn et al., 2007). In constructs with the photooxidant anthraquinone tethered to the DNA distally from the p53 response element, irradiation induced p53 dissociation in an artificial response element as measured in gel-shift assays. However, this p53 dissociation was not observed with an intervening C:A mismatch, implying a DNA-mediated process. Intriguingly, in natural p53 response elements, this p53 oxidation via DNA CT is sequence-specific. Promoter sequences for the p21 gene, encoding a protein involved in cell cycle arrest, and that for Gadd45, encoding a protein more involved in DNA repair, were compared using anthraquinone constructs. Dissociation of p53 from the Gadd45 response element was observed upon irradiation, which would serve to downregulate the gene inside cells, while little dissociation was observed from the p21 sequence. Under conditions of overwhelming oxidative stress within the cell, genes encoding proteins

stimulating DNA repair, such as Gadd45, would be downregulated in favor of those promoting cell cycle arrest and apoptotic pathways, such as p21. The sequence-specific DNA-mediated oxidation and dissociation of p53 provides a mechanism for how this could occur selectively.

Further work elucidated the important factors for the sequence selectivity of p53 dissociation (Schaefer and Barton, 2014). Again using anthraquinone constructs, artificial p53 response elements were created where the guanine content of a purine region within the response element was successively increased, essentially titrating the oxidation potential. Upon irradiation, a response element containing AAA displayed the lowest level of p53 dissociation, while a sequence with GGG showed the highest level of dissociation. Natural response element with similar guanine content behaved in the same way: S100A2 with GGG in its response element dissociated more upon irradiation than the caspase sequence with AGA. Thus p53 is preferentially dissociated when low potential guanine multiplets are located within the consensus sequence (Figure 8C). The relative importance of particular cysteine residues in the DNA-mediated oxidation of p53 was then explored by serine mutagenesis (Schaefer et al., 2015). The ability to dissociate from the Gadd45 promoter upon DNA-mediated oxidation was assayed for six cysteine to serine p53 mutants. The C275S and C277S mutations, located nearby the DNA interface, most significantly impaired protein dissociation. Mass spectrometry experiments then provided further insight by mapping the cysteine oxidation of specific residues through differential thiol labeling with iodoacetamide.

Thus DNA CT provides a compelling mechanism by which p53 can selectively dissociate from different consensus sequences within the cell under conditions of oxidative stress. Moreover, as evidenced by p53, proteins that contain redox-active cofactors other than iron-sulfur clusters can also participate in DNA-mediated processes.

Conclusions

Here we have examined how DNA CT involves the efficient transport of electrons or electron holes through the DNA π -stack over long molecular distances. Along with this shallow distance dependence, DNA CT is sensitive to mismatches or lesions that disrupt π -stacking and is critically dependent on proper electronic coupling of the donor and acceptor moieties into the base stack. Thus DNA CT provides a mechanism for probing the fidelity of the DNA. Favorable DNA CT is very rapid, occurring on the picosecond timescale. Because of this speed, electron holes equilibrate along the DNA π -stack, forming a characteristic pattern of DNA damage at low potential guanine multiplets. Electrochemical devices that take advantage of the characteristics of DNA CT have now been developed and shown to be competent to detect a variety of DNA-bound species and the activity of DNA binding enzymes, even from crude cell lysate. Therefore DNA CT provides a platform for rapid and simple DNA-based diagnostics.

More fundamentally, DNA CT may play specific biological roles especially in processes that we know must occur rapidly and over long distances within the cell such as genome surveillance. DNA processing enzymes with [4Fe4S] clusters can perform DNA-mediated

CT self-exchange reactions with other [4Fe4S] cluster proteins, even if the protein functions are quite dissimilar, as long as the DNA-bound [4Fe4S]^{3+/2+} redox potentials are conserved and the proteins are well coupled to the DNA to carry out CT. This chemistry thus enables a search of the genome for lesions and the coordinated signaling of a network of DNA repair enzymes containing [4Fe4S] clusters in seeking out those lesions. DNA CT chemistry also represents a means to protect the genome from oxidative damage, where the equilibrating electron holes within the DNA duplex may be intercepted by DNA-bound proteins, such as Dps, so as to protect the DNA library. DNA-bound redox-active transcription factors can also be activated from a distance through long range DNA CT, thereby providing a rapid response to an oxidative threat without the need for diffusion through the traffic of the cell.

Therefore DNA CT chemistry, sensitive to lesions and offering long-range signaling, provides a means of rapid communication across the genome. Given the increasing number of DNA-processing enzymes shown to contain redox-active moieties, it is tantalizing to consider the myriad ways DNA CT chemistry may be utilized. DNA-mediated signaling networks, facilitating coordination across the genome, await elucidation.

Acknowledgments

We are grateful to the NIH for their financial support and to all our coworkers and collaborators in this research. We also thank Dr. N. Muren for help with figures.

References

- Almirón M, Link AJ, Furlong D, Kolter R. A novel DNA-binding protein with regulatory and protective roles in starved *Escherichia coli*. *Genes Dev.* 1992; 6:2646–2654. [PubMed: 1340475]
- Arkin MR, Stemp ED, Holmlin RE, Barton JK, Hörmann A, Olson EJ, Barbara PF. Rates of DNA-mediated electron transfer between metallointercalators. *Science.* 1996; 273:475–480. [PubMed: 8662532]
- Arkin MR, Stemp ED, Pulver SC, Barton JK. Long-range oxidation of guanine by Ru(III) in duplex DNA. *Chem. Biol.* 1997; 4:389–400. [PubMed: 9195873]
- Arnold AR, Barton JK. DNA Protection by the Bacterial Ferritin Dps via DNA Charge Transport. *J. Am. Chem. Soc.* 2013; 135:15726–15729. [PubMed: 24117127]
- Augustyn KE, Merino EJ, Barton JK. A role for DNA-mediated charge transport in regulating p53: Oxidation of the DNA-bound protein from a distance. *Proc. Natl. Acad. Sci.* 2007; 104:18907–18912. [PubMed: 18025460]
- Baylin SB, Herman JG. DNA hypermethylation in tumorigenesis: epigenetics joins genetics. *Trends Genet. TIG.* 2000; 16:168–174. [PubMed: 10729832]
- Berlin YA, Burin AL, Ratner MA. Charge Hopping in DNA. *J. Am. Chem. Soc.* 2001; 123:260–268. [PubMed: 11456512]
- Blainey PC, Oijen AM, van Banerjee A, Verdine GL, Xie XS. A base-excision DNA-repair protein finds intrahelical lesion bases by fast sliding in contact with DNA. *Proc. Natl. Acad. Sci.* 2006; 103:5752–5757. [PubMed: 16585517]
- Boal AK, Barton JK. Electrochemical Detection of Lesions in DNA. *Bioconjug. Chem.* 2005; 16:312–321. [PubMed: 15769084]
- Boal AK, Yavin E, Lukianova OA, O'Shea VL, David SS, Barton JK. DNA-Bound Redox Activity of DNA Repair Glycosylases Containing [4Fe-4S] Clusters†. *Biochemistry (Mosc.)*. 2005; 44:8397–8407.
- Boal AK, Genereux JC, Sontz PA, Gralnick JA, Newman DK, Barton JK. Redox signaling between DNA repair proteins for efficient lesion detection. *Proc. Natl. Acad. Sci.* 2009; 106:15237–15242. [PubMed: 19720997]

- Boon EM, Ceres DM, Drummond TG, Hill MG, Barton JK. Mutation detection by electrocatalysis at DNA-modified electrodes. *Nat. Biotechnol.* 2000; 18:1096–1100. [PubMed: 11017050]
- Boon EM, Salas JE, Barton JK. An electrical probe of protein-DNA interactions on DNA-modified surfaces. *Nat. Biotechnol.* 2002; 20:282–286. [PubMed: 11875430]
- Boon EM, Jackson NM, Wightman MD, Kelley SO, Hill MG, Barton JK. Intercalative Stacking: A Critical Feature of DNA Charge-Transport Electrochemistry. *J. Phys. Chem. B.* 2003a; 107:11805–11812.
- Boon EM, Livingston AL, Chmiel NH, David SS, Barton JK. DNA-mediated charge transport for DNA repair. *Proc. Natl. Acad. Sci.* 2003b; 100:12543–12547. [PubMed: 14559969]
- Boubakri H, Septenville AL, de Viguera E, Michel B. The helicases DinG, Rep and UvrD cooperate to promote replication across transcription units in vivo. *EMBO J.* 2010; 29:145–157. [PubMed: 19851282]
- Ceci P, Cellai S, Falvo E, Rivetti C, Rossi GL, Chiancone E. DNA condensation and self-aggregation of *Escherichia coli* Dps are coupled phenomena related to the properties of the N-terminus. *Nucleic Acids Res.* 2004; 32:5935–5944. [PubMed: 15534364]
- Chaban Y, Boekema EJ, Dudkina NV. Structures of mitochondrial oxidative phosphorylation supercomplexes and mechanisms for their stabilisation. *Biochim. Biophys. Acta BBA - Bioenerg.* 2014; 1837:418–426.
- Cho Y, Gorina S, Jeffrey PD, Pavletich NP. Crystal structure of a p53 tumor suppressor-DNA complex: understanding tumorigenic mutations. *Science.* 1994; 265:346–355. [PubMed: 8023157]
- Cunningham RP, Asahara H, Bank JF, Scholes CP, Salerno JC, Surerus K, Munck E, McCracken J, Peisach J, Emptage MH. Endonuclease III is an iron-sulfur protein. *Biochemistry (Mosc.)*. 1989; 28:4450–4455.
- Das PM, Singal R. DNA methylation and cancer. *J. Clin. Oncol. Off. J. Am. Soc. Clin. Oncol.* 2004; 22:4632–4642.
- David SS, O'Shea VL, Kundu S. Base-excision repair of oxidative DNA damage. *Nature.* 2007; 447:941–950. [PubMed: 17581577]
- Demple B, Harrison L. Repair of Oxidative Damage to DNA: Enzymology and Biology. *Annu. Rev. Biochem.* 1994; 63:915–948. [PubMed: 7979257]
- Drummond TG, Hill MG, Barton JK. Electron Transfer Rates in DNA Films as a Function of Tether Length. *J. Am. Chem. Soc.* 2004; 126:15010–15011. [PubMed: 15547981]
- Elias B, Shao F, Barton JK. Charge Migration along the DNA Duplex: Hole versus Electron Transport. *J. Am. Chem. Soc.* 2008; 130:1152–1153. [PubMed: 18183988]
- Esteller M. CpG island hypermethylation and tumor suppressor genes: a booming present, a brighter future. *Oncogene.* 2002; 21:5427–5440. [PubMed: 12154405]
- Friedman AE, Chambron JC, Sauvage JP, Turro NJ, Barton JK. A molecular light switch for DNA: Ru(bpy)₂(dppz)²⁺. *J. Am. Chem. Soc.* 1990; 112:4960–4962.
- Friedman JI, Stivers JT. Detection of Damaged DNA Bases by DNA Glycosylase Enzymes. *Biochemistry.* 2010; 49:4957–4967. [PubMed: 20469926]
- Fromme JC, Banerjee A, Huang SJ, Verdine GL. Structural basis for removal of adenine mispaired with 8-oxoguanine by MutY adenine DNA glycosylase. *Nature.* 2004; 427:652–656. [PubMed: 14961129]
- Fujikawa M, Kobayashi K, Kozawa T. Direct oxidation of the [2Fe-2S] cluster in SoxR protein by superoxide: distinct differential sensitivity to superoxide-mediated signal transduction. *J. Biol. Chem.* 2012; 287:35702–35708. [PubMed: 22908228]
- Fukuzumi S, Miyao H, Ohkubo K, Suenobu T. Electron-transfer oxidation properties of DNA bases and DNA oligomers. *J. Phys. Chem. A.* 2005; 109:3285–3294. [PubMed: 16833661]
- Furst AL, Barton JK. DNA Electrochemistry Shows DNMT1 Methyltransferase Hyperactivity in Colorectal Tumors. *Chem. Biol.* 2015; 22:938–945. [PubMed: 26120002]
- Furst AL, Hill MG, Barton JK. DNA-Modified Electrodes Fabricated Using Copper-Free Click Chemistry for Enhanced Protein Detection. *Langmuir.* 2013; 29:16141–16149. [PubMed: 24328347]

- Furst AL, Muren NB, Hill MG, Barton JK. Label-free electrochemical detection of human methyltransferase from tumors. *Proc. Natl. Acad. Sci.* 2014; 111:14985–14989. [PubMed: 25288757]
- Fuss JO, Tsai C-L, Ishida JP, Tainer JA. Emerging critical roles of Fe-S clusters in DNA replication and repair. *Biochim. Biophys. Acta BBA - Mol. Cell Res.* 2015; 1853:1253–1271.
- Genereux JC, Augustyn KE, Davis ML, Shao F, Barton JK. Dependence of DNA-Mediated Charge Transport across Adenine Tracts. *J. Am. Chem. Soc.* 2008; 130:15150–15156. [PubMed: 18855390]
- Genereux JC, Barton JK. Mechanisms for DNA Charge Transport. *Chem. Rev.* 2010; 110:1642–1662. [PubMed: 20214403]
- Genereux JC, Wuerth SM, Barton JK. Single-Step Charge Transport through DNA over Long Distances. *J. Am. Chem. Soc.* 2011; 133:3863–3868. [PubMed: 21348520]
- Giese B, Amaudrut J, Köhler A-K, Spormann M, Wessely S. Direct observation of hole transfer through DNA by hopping between adenine bases and by tunneling. *Nature.* 2001; 412:318–320. [PubMed: 11460159]
- Gorodetsky AA, Barton JK. Electrochemistry Using Self-Assembled DNA Monolayers on Highly Oriented Pyrolytic Graphite. *Langmuir.* 2006; 22:7917–7922. [PubMed: 16922584]
- Gorodetsky AA, Boal AK, Barton JK. Direct Electrochemistry of Endonuclease III in the Presence and Absence of DNA. *J. Am. Chem. Soc.* 2006; 128:12082–12083. [PubMed: 16967954]
- Gorodetsky AA, Green O, Yavin E, Barton JK. Coupling into the Base Pair Stack Is Necessary for DNA-Mediated Electrochemistry. *Bioconjug. Chem.* 2007; 18:1434–1441. [PubMed: 17580927]
- Gorodetsky AA, Ebrahim A, Barton JK. Electrical Detection of TATA Binding Protein at DNA-Modified Microelectrodes. *J. Am. Chem. Soc.* 2008a; 130:2924–2925. [PubMed: 18271589]
- Gorodetsky AA, Dietrich LEP, Lee PE, Demple B, Newman DK, Barton JK. DNA binding shifts the redox potential of the transcription factor SoxR. *Proc. Natl. Acad. Sci.* 2008b; 105:3684–3689. [PubMed: 18316718]
- Grodick MA, Segal HM, Zwang TJ, Barton JK. DNA-Mediated Signaling by Proteins with 4Fe-4S Clusters Is Necessary for Genomic Integrity. *J. Am. Chem. Soc.* 2014; 136:6470–6478. [PubMed: 24738733]
- Grodick MA, Muren NB, Barton JK. DNA Charge Transport within the Cell. *Biochemistry.* 2015; 54:962–973. [PubMed: 25606780]
- Gu M, Imlay JA. The SoxRS response of *Escherichia coli* is directly activated by redox-cycling drugs rather than by superoxide. *Mol. Microbiol.* 2011; 79:1136–1150. [PubMed: 21226770]
- Guo X, Gorodetsky AA, Hone J, Barton JK, Nuckolls C. Conductivity of a single DNA duplex bridging a carbon nanotube gap. *Nat. Nanotechnol.* 2008; 3:163–167. [PubMed: 18654489]
- Hall DB, Barton JK. Sensitivity of DNA-Mediated Electron Transfer to the Intervening π -Stack: A Probe for the Integrity of the DNA Base Stack. *J. Am. Chem. Soc.* 1997; 119:5045–5046.
- Hall DB, Holmlin RE, Barton JK. Oxidative DNA damage through long-range electron transfer. *Nature.* 1996; 382:731–735. [PubMed: 8751447]
- Halsey TA, Vazquez-Torres A, Gravdahl DJ, Fang FC, Libby SJ. The ferritin-like Dps protein is required for *Salmonella enterica* serovar Typhimurium oxidative stress resistance and virulence. *Infect. Immun.* 2004; 72:1155–1158. [PubMed: 14742565]
- Hirata A, Klein BJ, Murakami KS. The X-ray crystal structure of RNA polymerase from Archaea. *Nature.* 2008; 451:851–854. [PubMed: 18235446]
- Holmlin RE, Dandliker PJ, Barton JK. Synthesis of metallointercalator-DNA conjugates on a solid support. *Bioconjug. Chem.* 1999; 10:1122–1130. [PubMed: 10563783]
- Imlay JA. Cellular defenses against superoxide and hydrogen peroxide. *Annu. Rev. Biochem.* 2008; 77:755–776. [PubMed: 18173371]
- Kawai K, Majima T. Hole Transfer Kinetics of DNA. *Acc. Chem. Res.* 2013; 46:2616–2625. [PubMed: 23805774]
- Kelley SO, Holmlin RE, Stemp EDA, Barton JK. Photoinduced Electron Transfer in Ethidium-Modified DNA Duplexes: Dependence on Distance and Base Stacking. *J. Am. Chem. Soc.* 1997a; 119:9861–9870.

- Kelley SO, Barton JK, Jackson NM, Hill MG. Electrochemistry of Methylene Blue Bound to a DNA-Modified Electrode. *Bioconjug. Chem.* 1997b; 8:31–37. [PubMed: 9026032]
- Kelley SO, Boon EM, Barton JK, Jackson NM, Hill MG. Single-base mismatch detection based on charge transduction through DNA. *Nucleic Acids Res.* 1999; 27:4830–4837. [PubMed: 10572185]
- Kim Y-J, Wilson DM. Overview of base excision repair biochemistry. *Curr. Mol. Pharmacol.* 2012; 5:3–13. [PubMed: 22122461]
- Krapp AR, Humbert MV, Carrillo N. The soxRS response of *Escherichia coli* can be induced in the absence of oxidative stress and oxygen by modulation of NADPH content. *Microbiol. Read. Engl.* 2011; 157:957–965.
- Lee PE, Demple B, Barton JK. DNA-mediated redox signaling for transcriptional activation of SoxR. *Proc. Natl. Acad. Sci. U. S. A.* 2009; 106:13164–13168. [PubMed: 19651620]
- Lewis FD, Kalgutkar RS, Wu Y, Liu X, Liu J, Hayes RT, Miller SE, Wasielewski MR. Driving Force Dependence of Electron Transfer Dynamics in Synthetic DNA Hairpins. *J. Am. Chem. Soc.* 2000; 122:12346–12352.
- Li X, Pal U, Ramamoorthi N, Liu X, Desrosiers DC, Eggers CH, Anderson JF, Radolf JD, Fikrig E. The Lyme disease agent *Borrelia burgdorferi* requires BB0690, a Dps homologue, to persist within ticks. *Mol. Microbiol.* 2007; 63:694–710. [PubMed: 17181780]
- Liu T, Barton JK. DNA Electrochemistry through the Base Pairs Not the Sugar-Phosphate Backbone. *J. Am. Chem. Soc.* 2005; 127:10160–10161. [PubMed: 16028914]
- Mui TP, Fuss JO, Ishida JP, Tainer JA, Barton JK. ATP-Stimulated, DNA-Mediated Redox Signaling by XPD, a DNA Repair and Transcription Helicase. *J. Am. Chem. Soc.* 2011; 133:16378–16381. [PubMed: 21939244]
- Muren NB, Barton JK. Electrochemical Assay for the Signal-On Detection of Human DNA Methyltransferase Activity. *J. Am. Chem. Soc.* 2013; 135:16632–16640. [PubMed: 24164112]
- Murphy CJ, Arkin MR, Jenkins Y, Ghatlia ND, Bossmann SH, Turro NJ, Barton JK. Long-range photoinduced electron transfer through a DNA helix. *Science.* 1993; 262:1025–1029. [PubMed: 7802858]
- Netz DJA, Stith CM, Stümpfig M, Köpf G, Vogel D, Genau HM, Stodola JL, Lill R, Burgers PMJ, Pierik AJ. Eukaryotic DNA polymerases require an iron-sulfur cluster for the formation of active complexes. *Nat. Chem. Biol.* 2012; 8:125–132. [PubMed: 22119860]
- Núñez ME, Noyes KT, Barton JK. Oxidative Charge Transport through DNA in Nucleosome Core Particles. *Chem. Biol.* 2002; 9:403–415. [PubMed: 11983330]
- Olmon ED, Hill MG, Barton JK. Using Metal Complex Reduced States to Monitor the Oxidation of DNA. *Inorg. Chem.* 2011; 50:12034–12044. [PubMed: 22043853]
- Olsen KN, Larsen MH, Gahan CGM, Kallipolitis B, Wolf XA, Rea R, Hill C, Ingmer H. The Dps-like protein Fri of *Listeria monocytogenes* promotes stress tolerance and intracellular multiplication in macrophage-like cells. *Microbiol. Read. Engl.* 2005; 151:925–933.
- O'Neill MA, Barton JK. DNA Charge Transport: Conformationally Gated Hopping through Stacked Domains. *J. Am. Chem. Soc.* 2004; 126:11471–11483. [PubMed: 15366893]
- Pang B, Hong W, Kock ND, Swords WE. Dps promotes survival of nontypeable *Haemophilus influenzae* in biofilm communities in vitro and resistance to clearance in vivo. *Front. Cell. Infect. Microbiol.* 2012; 2:58. [PubMed: 22919649]
- Pheaney CG, Barton JK. DNA Electrochemistry with Tethered Methylene Blue. *Langmuir.* 2012; 28:7063–7070. [PubMed: 22512327]
- Porello SL, Cannon MJ, David SS. A Substrate Recognition Role for the [4Fe-4S]²⁺ Cluster of the DNA Repair Glycosylase MutY. *Biochemistry (Mosc.).* 1998; 37:6465–6475.
- Rajski SR, Barton JK. How different DNA-binding proteins affect long-range oxidative damage to DNA. *Biochemistry (Mosc.).* 2001; 40:5556–5564.
- Ren B, Duan X, Ding H. Redox Control of the DNA Damage-inducible Protein DinG Helicase Activity via Its Iron-Sulfur Cluster. *J. Biol. Chem.* 2009; 284:4829–4835. [PubMed: 19074432]
- Renaud N, Berlin YA, Lewis FD, Ratner MA. Between Superexchange and Hopping: An Intermediate Charge-Transfer Mechanism in Poly(A)-Poly(T) DNA Hairpins. *J. Am. Chem. Soc.* 2013; 135:3953–3963. [PubMed: 23402652]

- Satin B, Del Giudice G, Della Bianca V, Dusi S, Laudanna C, Tonello F, Kelleher D, Rappuoli R, Montecucco C, Rossi F. The neutrophil-activating protein (HP-NAP) of *Helicobacter pylori* is a protective antigen and a major virulence factor. *J. Exp. Med.* 2000; 191:1467–1476. [PubMed: 10790422]
- Schaefer KN, Barton JK. DNA-Mediated Oxidation of p53. *Biochemistry (Mosc.)*. 2014; 53:3467–3475.
- Schaefer KN, Geil WM, Sweredoski MJ, Moradian A, Hess S, Barton JK. Oxidation of p53 through DNA Charge Transport Involves a Network of Disulfides within the DNA-Binding Domain. *Biochemistry (Mosc.)*. 2015; 54:932–941.
- Schuster GB. Long-Range Charge Transfer in DNA: Transient Structural Distortions Control the Distance Dependence. *Acc. Chem. Res.* 2000; 33:253–260. [PubMed: 10775318]
- Shao F, Barton JK. Long-range electron and hole transport through DNA with tethered cyclometalated iridium(III) complexes. *J. Am. Chem. Soc.* 2007; 129:14733–14738. [PubMed: 17985895]
- Slinker JD, Muren NB, Gorodetsky AA, Barton JK. Multiplexed DNA-Modified Electrodes. *J. Am. Chem. Soc.* 2010; 132:2769–2774. [PubMed: 20131780]
- Slinker JD, Muren NB, Renfrew SE, Barton JK. DNA charge transport over 34 nm. *Nat. Chem.* 2011; 3:228–233. [PubMed: 21336329]
- Sontz PA, Mui TP, Fuss JO, Tainer JA, Barton JK. DNA charge transport as a first step in coordinating the detection of lesions by repair proteins. *Proc. Natl. Acad. Sci.* 2012; 109:1856–1861. [PubMed: 22308447]
- Sugiyama H, Saito I. Theoretical Studies of GG-Specific Photocleavage of DNA via Electron Transfer: Significant Lowering of Ionization Potential and 5'-Localization of HOMO of Stacked GG Bases in B-Form DNA. *J. Am. Chem. Soc.* 1996; 118:7063–7068.
- Sund CJ, Rocha ER, Tzianabos AO, Tzinabos AO, Wells WG, Gee JM, Reott MA, O'Rourke DP, Smith CJ. The *Bacteroides fragilis* transcriptome response to oxygen and H₂O₂: the role of OxyR and its effect on survival and virulence. *Mol. Microbiol.* 2008; 67:129–142. [PubMed: 18047569]
- Takada T, Barton JK. DNA charge transport leading to disulfide bond formation. *J. Am. Chem. Soc.* 2005; 127:12204–12205. [PubMed: 16131181]
- Theoret JR, Cooper KK, Zekarias B, Roland KL, Law BF, Curtiss R, Joens LA. The *Campylobacter jejuni* Dps homologue is important for in vitro biofilm formation and cecal colonization of poultry and may serve as a protective antigen for vaccination. *Clin. Vaccine Immunol. CVI.* 2012; 19:1426–1431. [PubMed: 22787197]
- Valis L, Wang Q, Raytchev M, Buchvarov I, Wagenknecht H-A, Fiebig T. Base pair motions control the rates and distance dependencies of reductive and oxidative DNA charge transfer. *Proc. Natl. Acad. Sci.* 2006; 103:10192–10195. [PubMed: 16801552]
- Voloshin ON, Vanevski F, Khil PP, Camerini-Otero RD. Characterization of the DNA Damage-inducible Helicase DinG from *Escherichia coli*. *J. Biol. Chem.* 2003; 278:28284–28293. [PubMed: 12748189]
- Vousden KH, Lu X. Live or let die: the cell's response to p53. *Nat. Rev. Cancer.* 2002; 2:594–604. [PubMed: 12154352]
- Wallace SS. DNA glycosylases search for and remove oxidized DNA bases. *Environ. Mol. Mutagen.* 2013; 54:691–704. [PubMed: 24123395]
- Wan C, Fiebig T, Kelley SO, Treadway CR, Barton JK, Zewail AH. Femtosecond dynamics of DNA-mediated electron transfer. *Proc. Natl. Acad. Sci.* 1999; 96:6014–6019. [PubMed: 10339533]
- Watanabe S, Kita A, Kobayashi K, Miki K. Crystal structure of the [2Fe-2S] oxidative-stress sensor SoxR bound to DNA. *Proc. Natl. Acad. Sci. U. S. A.* 2008; 105:4121–4126. [PubMed: 18334645]
- Weiner BE, Huang H, Dattilo BM, Nilges MJ, Fanning E, Chazin WJ. An Iron-Sulfur Cluster in the C-terminal Domain of the p58 Subunit of Human DNA Primase. *J. Biol. Chem.* 2007; 282:33444–33451. [PubMed: 17893144]
- Williams TT, Dohno C, Stemp EDA, Barton JK. Effects of the photooxidant on DNA-mediated charge transport. *J. Am. Chem. Soc.* 2004; 126:8148–8158. [PubMed: 15225056]
- Xiang L, Palma JL, Bruot C, Mujica V, Ratner MA, Tao N. Intermediate tunnelling-hopping regime in DNA charge transport. *Nat. Chem.* 2015; 7:221–226. [PubMed: 25698331]

- Yavin E, Boal AK, Stemp EDA, Boon EM, Livingston AL, O'Shea VL, David SS, Barton JK. Protein-DNA charge transport: Redox activation of a DNA repair protein by guanine radical. *Proc. Natl. Acad. Sci. U. S. A.* 2005; 102:3546–3551. [PubMed: 15738421]
- Yavin E, Stemp EDA, O'Shea VL, David SS, Barton JK. Electron trap for DNA-bound repair enzymes: A strategy for DNA-mediated signaling. *Proc. Natl. Acad. Sci. U. S. A.* 2006; 103:3610–3614. [PubMed: 16505354]
- Zeth K. Dps biomineralizing proteins: multifunctional architects of nature. *Biochem. J.* 2012; 445:297–311. [PubMed: 22788214]
- Zhao G, Ceci P, Ilari A, Giangiacomo L, Laue TM, Chiancone E, Chasteen ND. Iron and hydrogen peroxide detoxification properties of DNA-binding protein from starved cells. A ferritin-like DNA-binding protein of *Escherichia coli*. *J. Biol. Chem.* 2002; 277:27689–27696. [PubMed: 12016214]

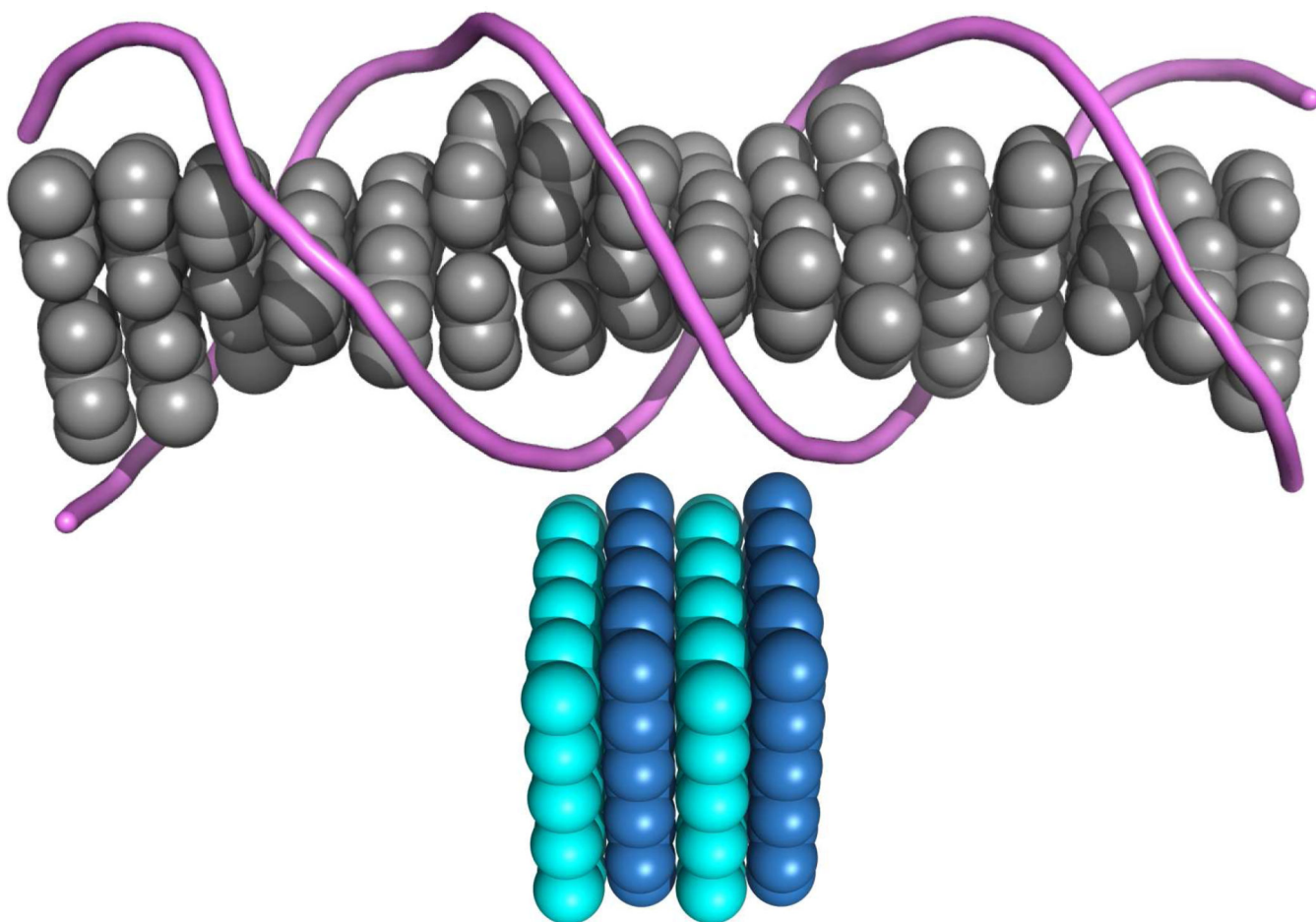


Figure 1. Comparison of DNA and graphite structures

Spacing between adjacent base pairs in DNA (3.4 Å) is similar to the planar spacing in graphite (z-direction). This close proximity of aromatic base-pairs allows for significant orbital overlap along the DNA helix, resulting in π -stacking of the DNA bases. The structural similarity between graphite, a known conductive material, and DNA was an initial clue to the conductivity of DNA. PDB file 3BSE (DNA).

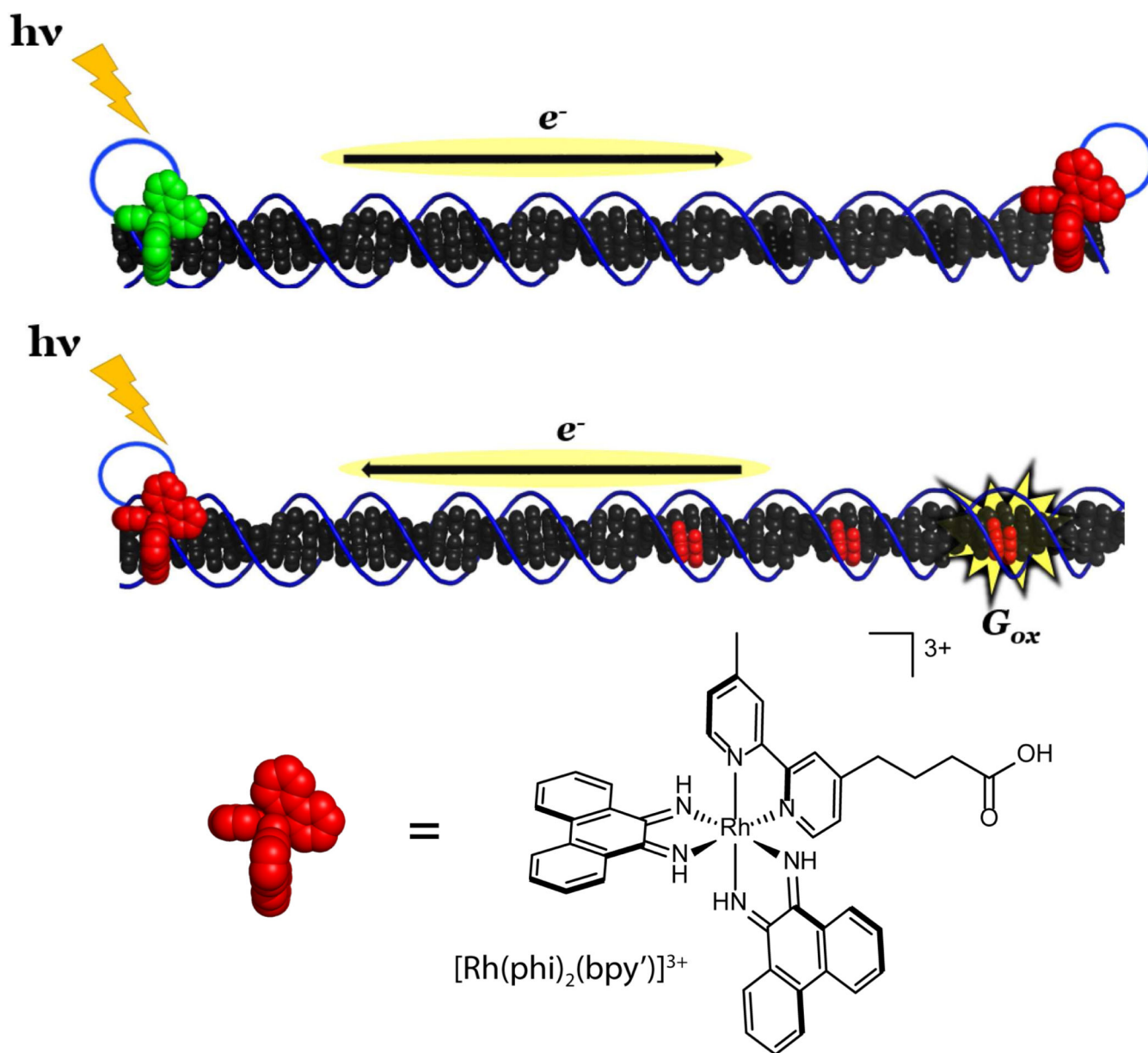


Figure 2. Solution platforms for studying DNA CT

Top: In the initial studies of DNA CT, electron transfer between metal complexes via the DNA could be detected by monitoring the quenching of the fluorescence from a tethered ruthenium metal complex (green) by a distally tethered rhodium complex (red). Bottom: DNA CT can also be detected by monitoring the oxidation of guanine by a tethered rhodium photooxidant (red) injecting holes into the DNA that localize to the distal guanines. Structure of an intercalating photooxidant $[Rh(\phi)_2(bpy')]^{2+}$ is shown.

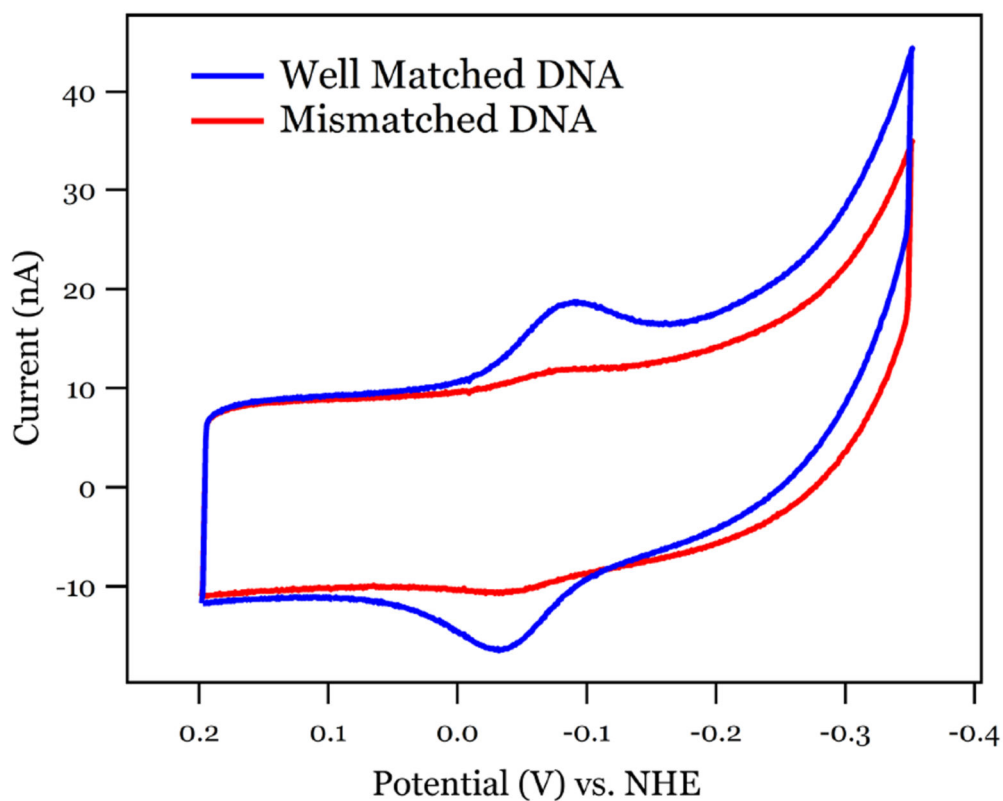
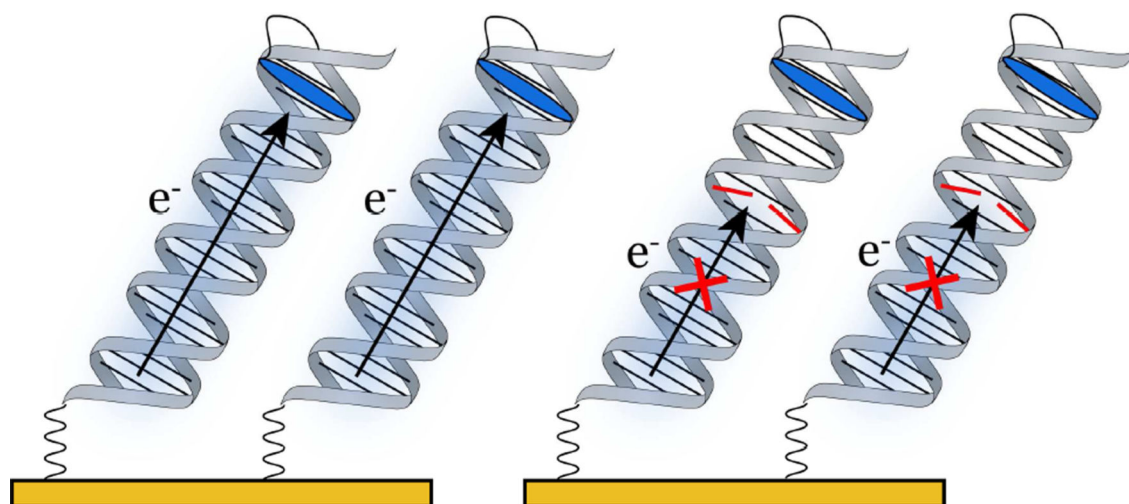


Figure 3. Mismatch detection on DNA-modified electrodes

Comparison of the electrochemical properties of a well-matched DNA monolayer assembled on gold electrodes to that of a monolayer containing a single base pair mismatch. A distally bound, covalent redox probe such as Nile blue can stack with the DNA bases and report on the integrity of the DNA. Cyclic voltammogram (CV) traces demonstrate that current flows from the electrode surface to the redox probe at different applied potentials in physiological buffer. Charge can flow efficiently through well-matched DNA, but when the π -stacking of

the bases is disrupted by a single base pair mismatch or lesion, DNA CT is attenuated and current does not flow effectively to the redox probe.

Author Manuscript

Author Manuscript

Author Manuscript

Author Manuscript

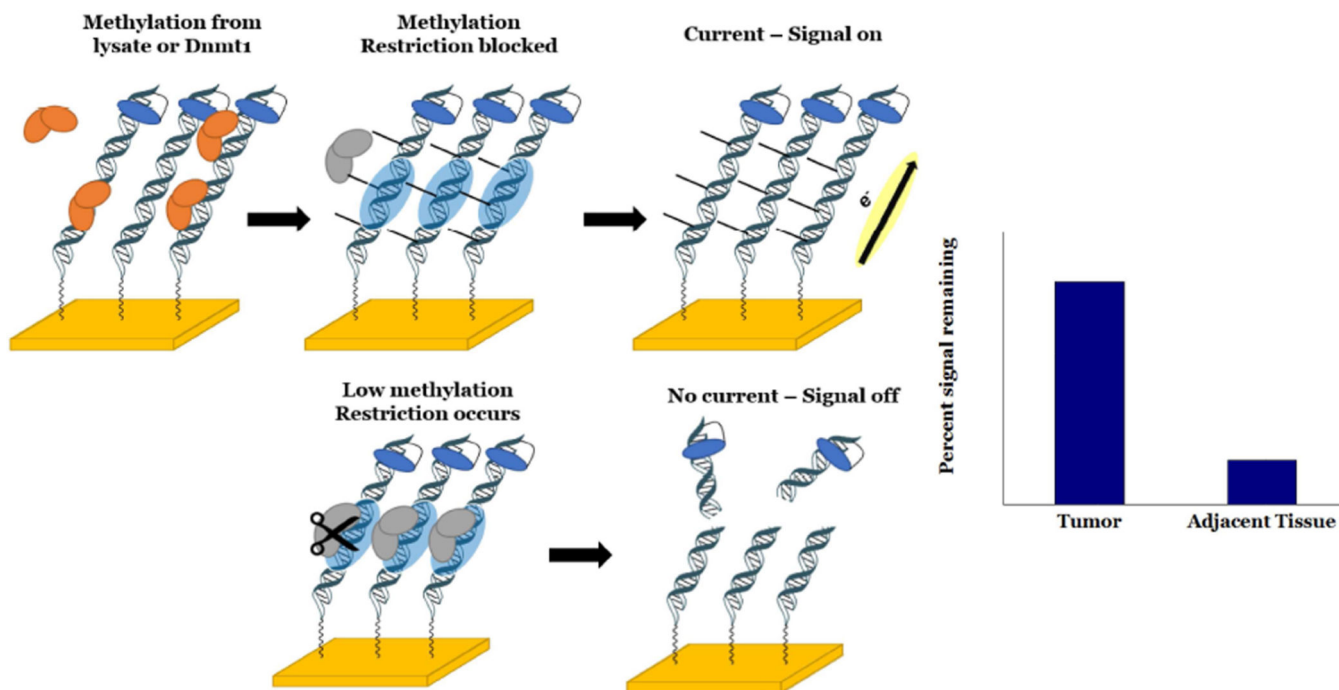


Figure 4. Electrochemical assay for the detection of methyltransferase activity

A self-assembled monolayer of DNA tethered to methylene blue on a gold electrode can be used to measure the methyltransferase activity of assayed solutions. The electrode is first treated with either purified methyltransferases, such as human Dnmt1, or lysates from tumors. If the DNA is not fully methylated, then a restriction enzyme can cut the DNA at a restriction site, highlighted in blue, within the DNA. After washing, the electrochemical signal is turned off, leading to a low percent of signal remaining compared to the signal before treatment with the restriction enzyme. If the DNA is methylated, corresponding to high methyltransferase activity, then the DNA is protected from restriction and the electrochemical signal is unperturbed, corresponding to a high percent of signal remaining. This assay has been used to detect the methyltransferase activity from tumor lysates (right). For tumor lysates tested with this device, the percent of signal remaining after treatment with restriction enzymes is high owing to increased methyltransferase activity. Lysates from adjacent tissue, however, have low percent signal remaining. Thus, lysates from tumors and normal tissue can be distinguished using this assay.

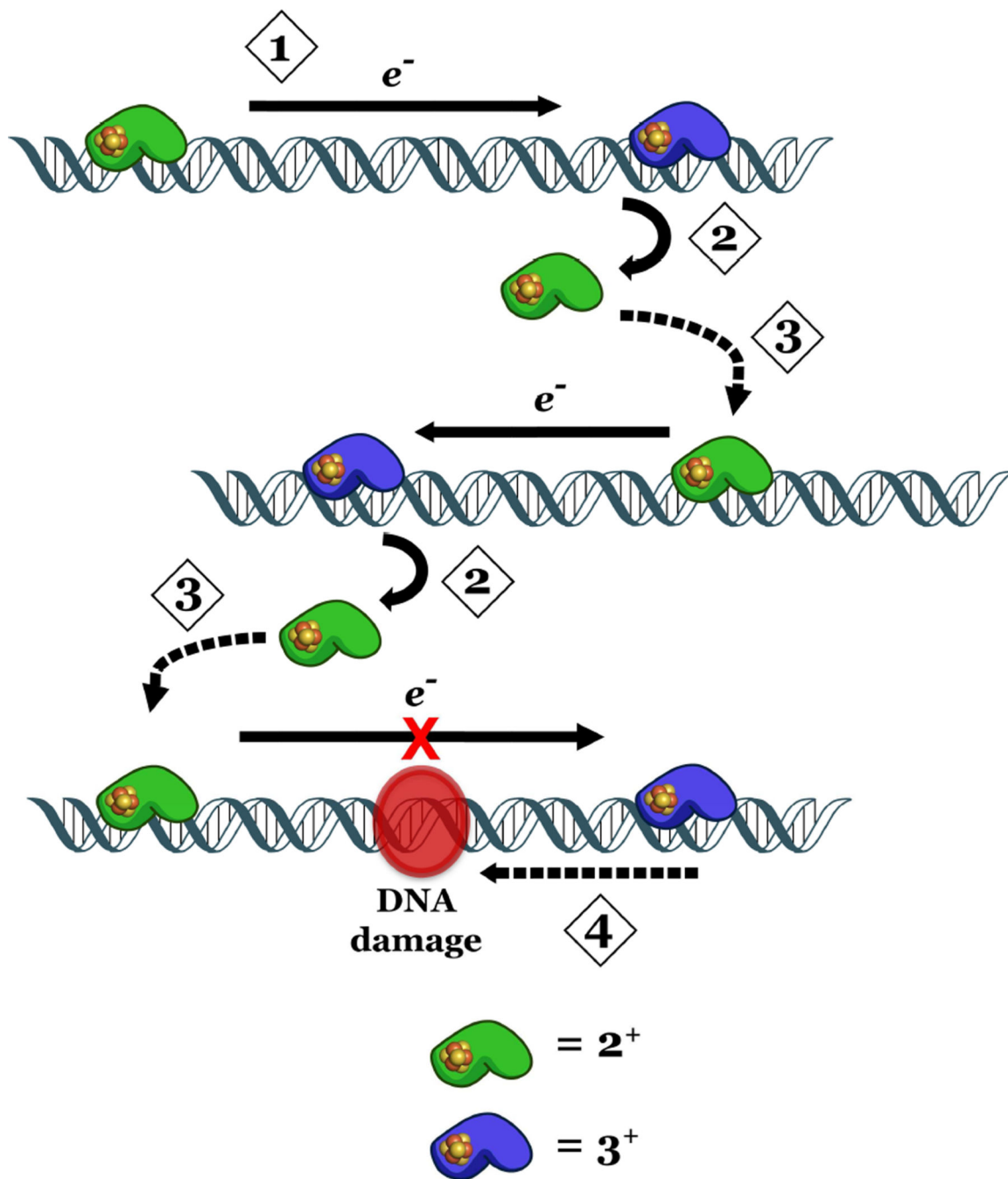


Figure 5. Redistribution of DNA repair proteins to sites of damage via DNA-mediated CT signaling

Diffusing DNA-processing enzymes with 4Fe-4S clusters such as EndoIII, MutY, or DinG bind to DNA in the 2+ oxidation state (green) [1]. An electron can be transferred to a nearby oxidized protein in the 3+ oxidation state (blue), reducing it to the 2+ oxidation state, promoting its dissociation from DNA owing to a decreased binding affinity [2]. The protein can then take advantage of 3D diffusion in order to search the genome elsewhere for damage [3]. If there is an intervening lesion or substrate that attenuates or blocks DNA CT such as a DNA lesion or R-loop, the proteins stay bound to the DNA and use 1D diffusion to locate

the substrate to be processed [4]. This mechanism provides a means for proteins to locate DNA damage within a sea of undamaged bases in the genome.

Author Manuscript

Author Manuscript

Author Manuscript

Author Manuscript

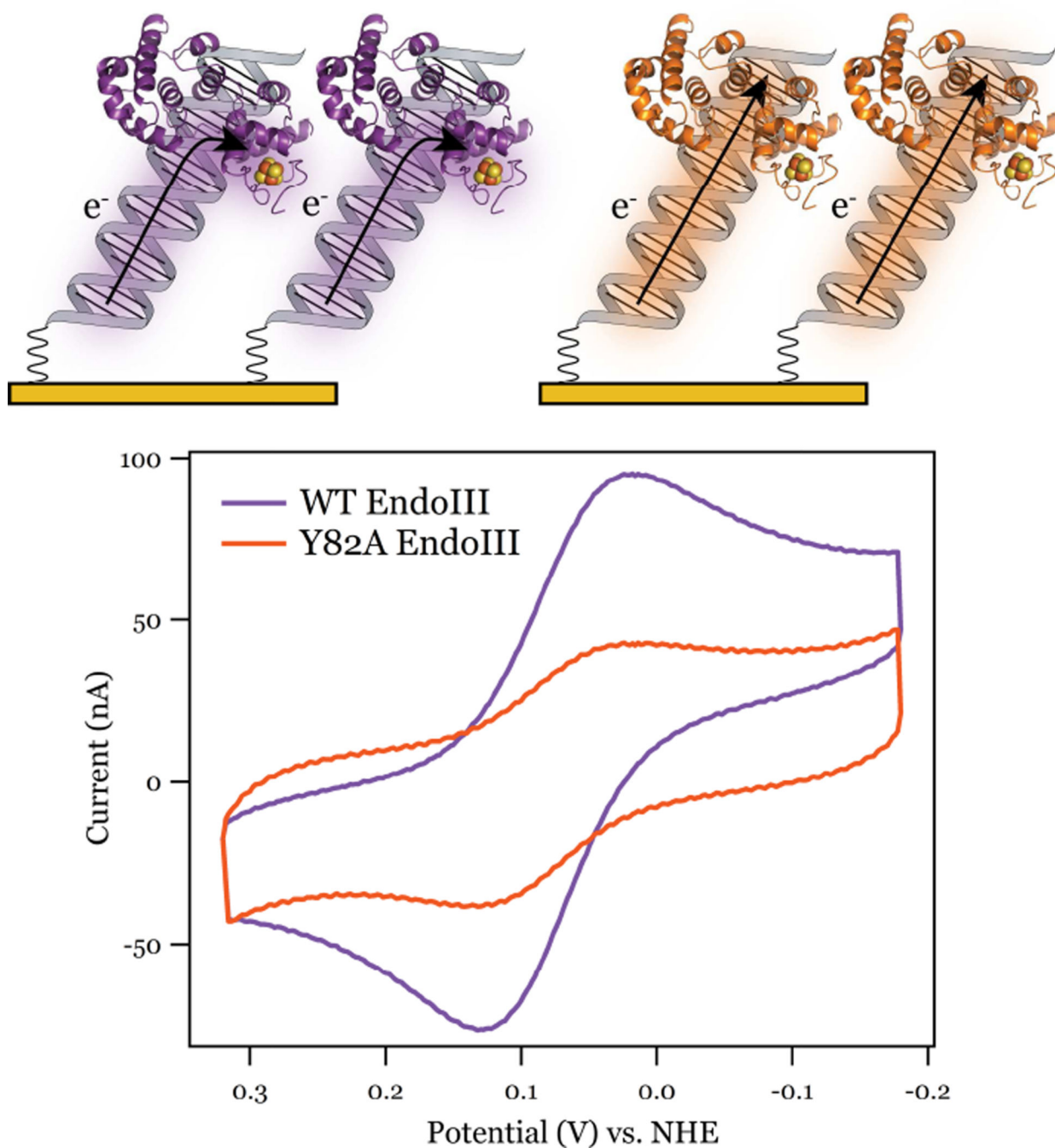


Figure 6. DNA electrochemistry of WT and Y82A EndoIII

DNA-binding proteins with redox-active cofactors such as iron-sulfur clusters can be assayed on DNA-modified electrodes, effectively measuring their DNA-bound redox potentials. DNA binding shifts the redox potential of the $[4\text{Fe}4\text{S}]^{3+/2+}$ couple of the base excision repair protein EndoIII, activating the protein towards oxidation. The EndoIII mutant Y82A is less proficient in DNA charge transfer electrochemically, with less charge passing from the DNA through the protein to the cluster. Thus Y82A EndoIII is less able to

cooperate with other iron-sulfur cluster proteins via DNA CT to scan the genome for damage.

Author Manuscript

Author Manuscript

Author Manuscript

Author Manuscript

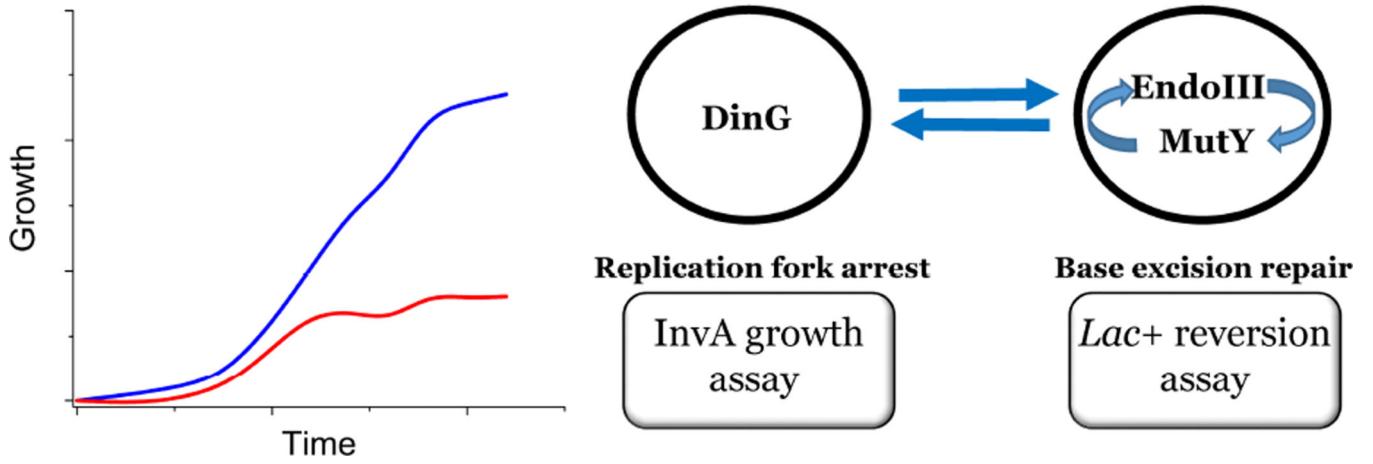


Figure 7. Genetic experiments indicate DNA-mediated signaling among DinG, EndoIII, and MutY

Left: When EndoIII is knocked out of *InvA* cells that depend upon R-loop repair by DinG for growth, a significant growth defect is observed (red). When the knockout, *InvA nth*, is complemented with a plasmid encoding WT EndoIII, EndoIII D138A, or RNaseH growth is restored (blue). When *InvA nth* is complemented with an empty plasmid or a plasmid encoding EndoIII Y82A, the growth defect remains (red). Taken together this indicates that the growth defect is indeed due to silencing the *nth* gene, that there is signaling between EndoIII and DinG to facilitate the unwinding of R-loops, and that this signaling is DNA-mediated; the enzymatically active but CT-deficient mutant EndoIII Y82A cannot restore growth while the CT-proficient but catalytically inactive EndoIII D138A does restore growth. Right: The *InvA* growth assay and *Lac+* reversion assays tested indicate that DNA-mediated signaling facilitates signaling among DinG, EndoIII, and MutY.

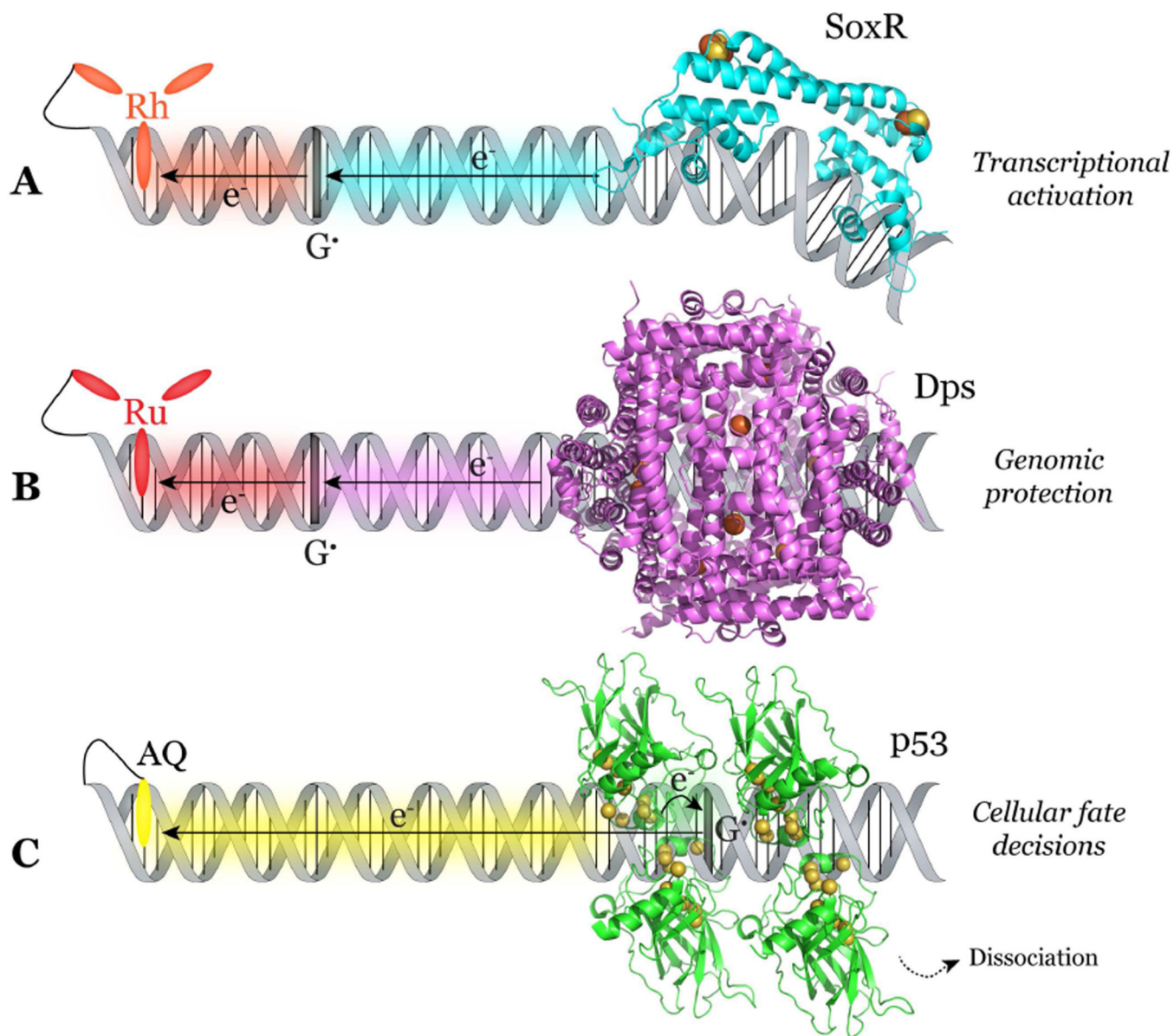


Figure 8. SoxR, Dps and p53 proteins use DNA CT to sense and respond to distant DNA damage produced by a tethered photooxidant

(A) SoxR, a bacterial transcription factor involved in response to superoxide stress, contains $[2\text{Fe}2\text{S}]^{2+/1+}$ clusters and undergoes a conformational change and transcriptional activation upon oxidation. Irradiation of a construct with covalently tethered photooxidant $[\text{Rh}(\text{phi})_2(\text{bpy}')]^{3+}$ located 80 base pairs from the SoxR promoter binding site produced *soxS*, the target gene for SoxR. Irradiation of the photooxidant produces an excited state capable of oxidizing DNA, the injected electron hole localizes to guanine radicals, and SoxR then becomes oxidized to fill guanine radicals, resulting in transcriptional activation from a distance via DNA CT. (B) Dps proteins, bacterial mini ferritins implicated in the virulence of pathogenic bacteria, contain iron-binding ferroxidase sites and are involved in DNA protection from oxidative stress. Damage created at a low redox potential guanine triplet upon irradiation with tethered photooxidant $[\text{Ru}(\text{phen})(\text{dppz})(\text{bpy}')]^{2+}$ can be attenuated by

Dps loaded with ferrous iron, but not by Apo-Dps or Dps loaded with ferric iron, which both lack reducing equivalents. Charge transfer from the ferrous iron bound at the ferroxidase sites of Dps to guanine radical holes within DNA could be an efficient mechanism of genomic protection from a distance via DNA CT. (C) p53, a human transcription factor known as the “guardian of the genome”, contains a network of redox-active cysteine residues. Irradiation of constructs with a tethered anthraquinone photooxidant separated from the p53 response element can result in oxidation of these cysteine residues and dissociation of p53 from the DNA. Specifically, when the response element contains low redox potential guanine sites, p53 can become efficiently oxidized via DNA CT, resulting in decisions regarding the cellular fate. PDB files: SoxR (2ZHG), Dps (1N1Q), p53 (3KMD).